Clinical Cancer Research

Orally Bioavailable Androgen Receptor Degrader, Potential Next-Generation Therapeutic for Enzalutamide-Resistant Prostate Cancer

Suriyan Ponnusamy[1], Yali He[2], Dong-Jin Hwang[2], Thirumagal Thiyagarajan[1], Rene Houtman[3], Vera Bocharova[4], Bobby G. Sumpter[4], Elias Fernandez[5], Daniel Johnson[6], Ziyun Du[7], Lawrence M. Pfeffer[7], Robert H. Getzenberg[8], Iain J. McEwan[9], Duane D. Miller[2], and Ramesh Narayanan[1,10]

Abstract

Purpose: Androgen receptor (AR)-targeting prostate cancer drugs, which are predominantly competitive ligand-binding domain (LBD)-binding antagonists, are inactivated by common resistance mechanisms. It is important to develop next-generation mechanistically distinct drugs to treat castration- and drug-resistant prostate cancers.

Experimental Design: Second-generation AR pan antagonist UT-34 was selected from a library of compounds and tested in competitive AR binding and transactivation assays. UT-34 was tested using biophysical methods for binding to the AR activation function-1 (AF-1) domain. Western blot, gene expression, and proliferation assays were performed in various AR-positive enzalutamide-sensitive and -resistant prostate cancer cell lines. Pharmacokinetic and xenograft studies were performed in immunocompromised rats and mice.

Results: UT-34 inhibits the wild-type and LBD-mutant ARs comparably and inhibits the *in vitro* proliferation and *in vivo* growth of enzalutamide-sensitive and -resistant prostate cancer xenografts. In preclinical models, UT-34 induced the regression of enzalutamide-resistant tumors at doses when the AR is degraded; but, at lower doses, when the AR is just antagonized, it inhibits, without shrinking, the tumors. This indicates that degradation might be a prerequisite for tumor regression. Mechanistically, UT-34 promotes a conformation that is distinct from the LBD-binding competitive antagonist enzalutamide and degrades the AR through the ubiquitin proteasome mechanism. UT-34 has a broad safety margin and exhibits no cross-reactivity with G-protein–coupled receptor kinase and nuclear receptor family members.

Conclusions: Collectively, UT-34 exhibits the properties necessary for a next-generation prostate cancer drug.

Introduction

About 3.3 million men are presently living with prostate cancer in the United States and this number is expected to increase to 4.5 million by 2026 (1). In addition to radical prostatectomy combined with gonadotrophins, androgen-synthesizing enzyme inhibitor and androgen receptor (AR) antagonists have been the mainstay of prostate cancer treatment (2, 3). Prostate cancer that progresses after initial treatment (castration-resistant prostate cancer; CRPC), grows rapidly and metastasizes to distant organs (4, 5). Studies with targeted treatments (enzalutamide and apalutamide, AR antagonists, and abiraterone, an androgen-synthesizing enzyme inhibitor) that have been approved in the last 5–10 years to combat CRPC have provided clear evidence that CRPC, despite being castration-resistant, is still dependent on the AR axis for continued growth (2, 3).

About 30%–40% of CRPCs fail to respond to enzalutamide or abiraterone (2, 3, 6, 7), while the remaining CRPCs eventually develop resistance after a brief period of response (8). Although several potential mechanisms for resistance development have been identified, mutations in the AR ligand–binding domain (LBD), AR amplification, and expression of AR splice variants (AR-SV) have been broadly observed in the clinic (9, 10). AR antagonists currently in use (enzalutamide and apalutamide) and in clinical trials (darolutamide) are all competitive antagonists and their mechanisms of action are similar.

A member of the steroid receptor family of ligand-activated transcription factors, structurally, AR, like other steroid receptors, contains an N-terminus domain (NTD) that expresses an activation function (AF)-1 domain, a DNA-binding domain (DBD) that

[1]Department of Medicine, University of Tennessee Health Science Center, Memphis, Tennessee. [2]Department of Pharmaceutical Sciences, University of Tennessee Health Science Center, Memphis, Tennessee. [3]PamGene International, Den Bosch, the Netherlands. [4]Oak Ridge National Laboratory, Oak Ridge, Tennessee. [5]Biochemistry and Cell & Molecular Biology, University of Tennessee, Knoxville, Tennessee. [6]Molecular Bioinformatics Core, University of Tennessee Health Science Center, Memphis, Tennessee. [7]Department of Pathology, University of Tennessee Health Science Center, Memphis, Tennessee. [8]GTx, Inc., Memphis, Tennessee. [9]Institute of Medical Sciences, School of Medicine, Medical Sciences and Nutrition, University of Aberdeen, Aberdeen, Scotland, United Kingdom. [10]West Cancer Center, Memphis, Tennessee.

Note: Supplementary data for this article are available at Clinical Cancer Research Online (http://clincancerres.aacrjournals.org/).

Current address for R.H. Getzenberg: Dr. Kiran C. Patel College of Allopathic Medicine, Nova Southeastern University, Fort Lauderdale, Florida.

Corresponding Author: Ramesh Narayanan, University of Tennessee Health Science Center, Cancer Research Building, 19 South Manassas, Room 120, Memphis, TN 38103. Phone 901-448-2403; Fax: 901-448-3910; E-mail: rnaraya4@uthsc.edu

Clin Cancer Res 2019;25:6764–80

doi: 10.1158/1078-0432.CCR-19-1458

Translational Relevance

Conventional prostate cancer therapeutics are ligand-binding domain (LBD)-binding competitive androgen receptor (AR) antagonists. Mechanistically distinct new chemical entities that can provide sustained growth inhibition to the evolving forms of prostate cancer are required. Here, we describe the discovery and characterization of an AR degrader that inhibits the growth of prostate cancers that are not only sensitive but also resistant to competitive antagonists. Unlike competitive antagonists, the AR degrader inhibits the growth of prostate cancer xenografts grown in intact and castrated animals, suggesting that this agent can be used to treat both castration-resistant and androgen-dependent prostate cancer. With a broad safety margin, the molecule may offer a safe and effective treatment option for advanced prostate cancer.

recognizes hormone response elements, a hinge region, and an LBD that contains an AF-2 (11). The AF-1 contains two transcription activation regions, tau-1 and tau-5, which retain the majority of the AR function. Drugs that target the steroid receptors act by predominantly binding to the LBD. Prolonged treatment with AR antagonists results in mutations in the LBD, leading to resistance, that is, W741 mutation leads to bicalutamide resistance (12), and F876 mutation confers resistance to enzalutamide and apalutamide (9, 13, 14).

While mutations in the AR-LBD can be ideally overcome with antagonists that bind to the LBD in a distinct conformation, resistance due to AR-SVs confers a serious challenge due to the absence of the LBD. Current AR-targeting drugs that bind to the LBD will be unable to inhibit AR-SV function. AR-SVs have been shown to be responsible for aggressive CRPC phenotype, shorter overall survival, and failure of the cancer to respond to AR-targeted treatments or to chemotherapeutic agents (10, 15–18). Although most of the recent studies on prostate cancer resistance have focused on AR-SVs, other pathways are also considered to play roles in resistance development (19, 20).

Although degraders of estrogen receptor (ER) have been successfully discovered (21, 22), AR degraders have not yet been developed. Degraders confer the added advantage of preventing AR activation by alternate signaling pathways and by intratumoral androgens, and hence might provide a sustained treatment option for CRPC. Because it is unclear whether the AR and AR-SVs exist as heterodimers or as independent homodimer isoforms, it is yet to be determined whether degrading the full-length AR could contribute to the downregulation of the AR-SVs (23, 24). Discovery of proteolysis-targeting chimeras (PROTAC) and small molecules from our group has indicated that AR degraders could be developed using alternate strategies (25–28). However, PROTACs are large molecules with molecular weights greater than 1,000 Da and our first-generation molecules (27, 28) have poor oral bioavailability. It is also important to develop molecules that bind to domains other than the LBD (27, 29) to inhibit AR-SVs and to overcome resistance.

Here we report the discovery of a novel small-molecule pan-antagonist and degrader, UT-34, a second-generation molecule, that binds to the AR, and degrades enzalutamide-sensitive and -resistant ARs and AR-SVs. UT-34, which possesses appropriate pharmacokinetic properties, was effective in various *in vivo* models. UT-34 inhibited androgen-dependent tissues such as prostate and seminal vesicles in rats, and the growth of enzalutamide-resistant CRPC xenografts. UT-34 also induced tumor regression in intact immunocompromised rats, which has not been observed before with competitive antagonists potentially due to their inability to compete against the abundant circulating testosterone. These data provide the first evidence for the potential of an orally bioavailable AR degrader to treat advanced prostate cancer.

Materials and Methods

Reagents

The source of several reagents used in this article has been described previously (27, 28). The following reagents were purchased from the indicated manufacturers: ^{3}H-mibolerone and R1881 (Perkin Elmer); enzalutamide (MedKoo); Dual-luciferase and CellTiter-Glo assay reagents (Promega); AR (N20 and C19), mono-, and poly- ubiquitin (SC-8017), and glucocorticoid receptor (GR) antibodies (Santa Cruz Biotechnology); AR PG-21 antibody (Millipore); dihydrotestosterone (DHT), dexamethasone, glyceraldehyde 3-phosphate dehydrogenase (GAPDH) antibody, chelerythrine chloride, and cycloheximide (Sigma); progesterone receptor (PR), estrogen receptor (ER), phospho PAK, and phospho PKC antibodies (Cell Signaling Technology); bortezomib and PAK inhibitor PF3758309 (Selleck Chemicals); AR-V7 antibody and serum prostate-specific antigen (PSA) kit (Abcam); lipofectamine and TaqMan primers and probes and real-time PCR reagents (Life Technologies); hyaluronic acid (HA) antibody (Novus Biologicals); doxycycline and 17-AAG (Thermo Fisher Scientific); liver microsomes (Xenotech LLC); and proteasome inhibitor MG-132 (R&D Systems). On-target plus smart pool nonspecific and MDM2 siRNAs were obtained from Dharmacon (Thermo Fisher Scientific).

Cell culture

LNCaP, PC-3, HEK-293, ZR-75-1, MDA-MB-453, VCaP, 22RV1, and COS7 cell lines were procured from the ATCC and cultured in accordance with their recommendations. LNCaP cell line stably transfected with doxycycline-inducible AR-V7 was a kind gift from Dr. Nancy L. Weigel (Baylor College of Medicine, Houston, TX; refs. 30, 31). LNCaP95 prostate cancer cell line that expresses AR and AR-V7 was a kind gift from Dr. Alan Meeker (John Hopkins Medical Institute, Baltimore, MD; ref. 32). Enzalutamide-resistant LNCaP (MR49F) cells were a kind gift from Dr. Martin Gleave (University of British Columbia, Vancouver, British Columbia, Canada; ref. 33). Enzalutamide-resistant VCaP cells (MDVR) were licensed from Dr. Donald McDonnell (Duke University, Durham, NC). Patient-derived xenograft (PDX) line PC346C was a kind gift from Dr. W.M. van Weerden (Erasmus Medical Center, Rotterdam, the Netherlands; refs. 34, 35). All cell lines were authenticated by short terminal DNA repeat assay (Genetica).

Gene expression

RNA extraction and cDNA preparations were performed using Cells-to-Ct kit. Gene expression studies were performed using TaqMan probes on an ABI 7900 Real Time PCR System.

Growth assay

Growth assay was performed using CellTiter-Glo or Sulforhodamine blue (SRB) reagents.

Plasmid constructs and transient transfection

Plasmids (CMV hAR, AR-LBD, PR, GR, MR, ER, GRE-LUC, CMV-*Renilla* LUC, AR-AF-1, and AR-NTD plasmids) used in the study were described previously (27, 36, 37). Mouse AR, rat GR, GAA (GR-NTD, AR-DBD, and AR-LBD), and AGG (AR-NTD, GR-DBD and GR-LBD) were kind gifts from Dr. Diane Robins (University of Michigan Medical School, Ann Arbor, MI; ref. 38). Constructs dtau1 (tau-1 deleted AR), dtau5 (tau-5 deleted AR), and AR-NTD-DBD were kind gifts from Dr. Frank Claessens (KU Leuven, Leuven, Belgium; refs. 39, 40). Transfections were performed using Lipofectamine Reagent (Life Technologies).

Competitive ligand-binding assay

Ligand-binding assay with purified GST-tagged AR-LBD and whole-cell binding assays with ^{3}H-mibolerone were performed as described previously (27, 41). Briefly, COS7 cells were plated in 24-well plates at 100,000 cells/well in DMEM (without phenol red) supplemented with 5% charcoal dextran-stripped FBS (csFBS). Cells were transfected with the amounts of AR-LBD indicated in the figures. Cells were treated with a dose response of various compounds in the presence of ^{3}H-mibolerone. Cells were washed 4 hours after treatment with ice-cold PBS, and the intracellular proteins and ^{3}H- mibolerone were extracted using ice-cold 100% ethanol. Radioactivity was counted using a scintillation counter.

Western blotting and immunoprecipitation

Cells were plated in 60-mm dishes in growth medium. Medium was changed to the respective medium described in the figures and treated with compounds under various conditions. Protein extracts were prepared and Western blot was performed as described previously (36, 37). Immunoprecipitation was performed using protein A/G agarose.

Fluorescence polarization

Endogenous steady-state emission spectra were measured for His-AR-NTD and His-AR-AF-1–purified proteins as described previously (27, 29, 42).

Microarray assay for real-time coregulator–nuclear receptor interaction

Functional AR analysis in cell lysates was performed as described previously (43, 44). In short, compound-treated cells were harvested and lysed. Lysates, containing AR, were incubated on PamChip #88101 (PamGene) with 154 coregulator-derived NR-binding motifs, using three technical replicates (arrays) per lysate. AR binding was detected using a fluorescently labeled antibody and quantified using BioNavigator software (PamGene). Treatment-induced log-fold change of coregulator binding (modulation index) treatment and *P* value by Student *t* test, both versus vehicle treatment, were calculated using R software and used to assess compound-induced modulation of AR conformation.

Microarray

To determine the effect of UT-34 on global gene expression, microarray analysis was performed. MR49F cells were maintained in 1% charcoal-stripped serum–containing medium for 2 days. Medium was changed again and the cells were treated with vehicle, 0.1 nmol/L R1881 alone, or in combination with 10 μmol/L UT-34 ($n = 3$–4/group). At 24 hours after treatment, the cells were harvested, RNA extracted, and was subjected to microarray analysis [University of Tennessee Health Science Center (UTHSC) Molecular Resources Center, Memphis, TN]. Clariom S array was processed as described previously (27) and the data were analyzed using one-way ANOVA. Genes that exhibited greater than 1.5 fold change with a false discovery rate $q < 0.05$ were considered for further analysis. Ingenuity Pathway Analysis (IPA) was performed to determine the canonical pathway and the diseases represented by the enriched genes. The microarray data were deposited in Gene Expression Omnibus (GEO) database (accession number is GSE 133119).

Mice xenograft experiment

All animal studies were conducted under UTHSC Animal Care and Use Committee–approved protocols. Nonobese diabetic/severe combined immunodeficiency Gamma (NSG) mice were housed (5 animals per cage) and were allowed free access to water and commercial rodent chow. Cell line xenografts were performed in NSG mice as published previously (37, 45). MR49F cells were implanted subcutaneously in intact mice ($n = 8$–10/group). Tumors were measured twice or thrice weekly and the volume calculated using the formula length × width × width × 0.5236. Once the tumors reached 100–200 mm^3, the animals were castrated and the tumors were allowed to regrow as castration-resistant tumors. Once the tumors reached 200–300 mm^3 postcastration, the animals were randomized and treated orally with vehicle (polyethylene glycol-300: DMSO 85:15) or UT-34. Animals were sacrificed at the end of the study and the tumors were weighed and stored for further processing.

Rat xenograft experiments

Rat xenograft experiments were performed in SRG (Sprague Dawley-Rag2:IL2rg KO) rats at Hera Biolabs. Rats were inoculated subcutaneously with 1×10^7 cells (VCaP or MDVR) in 50% Matrigel. Once the tumors reached 1,000–3,000 mm^3, the animals were either randomized and treated (intact) or were castrated and the tumors were allowed to grow as CRPC. Once the tumors attained 2,000–3,000 mm^3, the animals were orally treated as indicated in the figures. Tumor volumes were recorded thrice weekly. Blood collection and body weight measurements were performed weekly. At sacrifice, tumors were weighed and stored for further analyses.

Hershberger assay

Male mice or rats (6–8 weeks old) were randomized into groups based on body weight. Animals were treated with drugs by oral administration as indicated in the figures for 4 or 14 days. Animals were sacrificed, prostate and seminal vesicles were weighed, and organ weights were normalized to body weight.

Metabolic stability, pharmacokinetics, safety, and cross-reactivity studies

Metabolic stability studies in microsomes from various species were conducted as described previously (27). Pharmacokinetic studies were conducted at Covance. Cross-reactivity of UT-34 with GPCRs, kinases, and nuclear receptors was evaluated at DiscoverX Eurofins.

Statistical analysis

Statistical analysis was performed using Prism (GraphPad). *t* test was used to analyze data from experiments containing two

groups, while one-way ANOVA was used to analyze data from experiments containing more than two groups. Appropriate *post-hoc* test was used to analyze data that demonstrated significance in ANOVA. Statistical significance is represented as *, $P < 0.05$; **, $P < 0.01$; ***, $P < 0.001$.

LC/MS-MS method to detect UT-34 and UT-34 synthetic scheme are presented in the Supplementary Methods.

Results

Our first-generation SARDs, UT-69 and UT-155, were excellent degraders with unique mechanistic properties (27). Unfortunately, their pharmacokinetic properties were not appropriate for further development. Oral administration of UT-155 in rats for 14 days failed to significantly inhibit the androgen-dependent seminal vesicles weight (Supplementary Fig. S1A). UT-155 when dosed orally failed to inhibit growth of enzalutamide-resistant LNCaP (MR49F) xenograft grown in castrated NSG mice (Supplementary Fig. S1B). Mouse and human liver microsome data also show rapid clearance and short half-life of UT-155 (Supplementary Fig. S1C). Hence, we continued our pursuit to develop molecules that retain the degradation and antagonistic characteristics of the first-generation molecules but with better pharmacokinetic properties. UT-34 (Fig. 1A), which satisfies these requirements, was selected from a library for further characterization to develop it as a treatment for enzalutamide-resistant CRPC.

UT-34 inhibits wild-type and mutant ARs comparably

UT-34 was first tested in a binding assay *in vitro* using purified AR-LBD binding assay (27). Below 100 μmol/L concentration, UT-34 failed to bind to the purified AR-LBD and displace 1 nmol/L ^{3}H-mibolerone (Fig. 1B, left). To verify the result obtained in purified AR-LBD, we performed whole-cell ligand-binding assays in COS7 cells transfected with AR-LBD and treated with a dose response of UT-34 in combination with 1 nmol/L ^{3}H-mibolerone. UT-34 displaced ^{3}H-mibolerone, although its binding was much weaker (inhibition observed only at 10 μmol/L) than that of enzalutamide or UT-155 (Fig. 1B, right). The 10-fold difference between purified AR-LBD and whole-cell binding assays could be due to many possibilities: potential

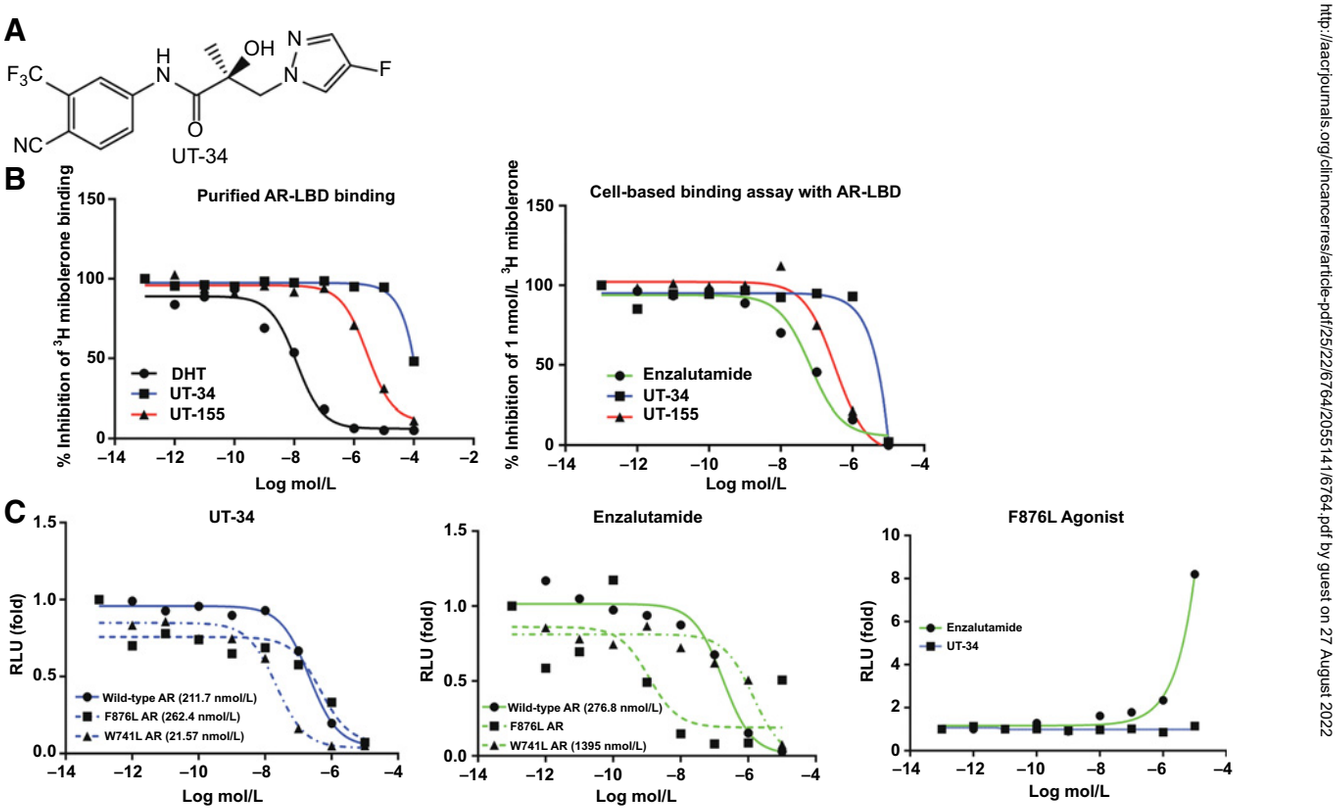

Figure 1.

Structure and properties of UT-34. **A,** Structure of UT-34. **B,** Left, UT-34 does not bind to the AR-LBD. Purified GST-tagged AR-LBD protein was incubated for 16 hours at 4°C with a dose response (1 pmol/L to 100 μmol/L) of the indicated compounds in the presence of 1 nmol/L ^{3}H -mibolerone. Unbound ^{3}H was washed and the bound ^{3}H was counted using a scintillation counter. **B,** Right, COS7 cells were transfected with 50 ng of AR-LBD. Cells were treated 48 hours after transfection with a dose response (1 pmol/L to 10 μmol/L) of the indicated compounds in the presence of 1 nmol/L ^{3}H-mibolerone for 4 hours. Unbound ^{3}H-mibolerone was washed with cold PBS and the bound ^{3}H was eluted with ice-cold ethanol. ^{3}H was counted using a scintillation counter. **C,** UT-34 comparably inhibits the transactivation of wild-type and mutant ARs. COS7 cells were transfected with 25 ng of cmv-hAR, hAR F876L, or hAR W741L, 0.25 μg GRE-LUC, and 10 ng CMV-*Renilla* LUC using lipofectamine. Cells were treated 24 hours after transfection with a dose response of UT-34 or enzalutamide in combination with 0.1 nmol/L R1881 (F876L agonist experiment was performed in the absence of 0.1 nmol/L R1881) and luciferase assay was performed 48 hours after transfection. Firefly luciferase was divided by *Renilla* luciferase. Values shown in the graphs are IC_{50} values. Experiments were performed at least $n = 3$ times and the representative graph is shown here. DHT, dihydrotestosterone; RLU, relative light units.

stabilization of the UT-34–AR–LBD complex by intracellular factors or faster on-off rate of UT-34 in the ligand-binding pocket in the absence of stabilization factors, or requirement of additional factors to bind to the AR-LBD. These questions need to be resolved in future studies.

We next determined the antagonistic property of UT-34 in wild-type and LBD-mutant ARs and compared the results to the effect of enzalutamide (Fig. 1C; Supplementary Table ST1). COS7 cells were transfected with wild-type or mutant ARs, GRE-LUC, and CMV-*Renilla* LUC and a luciferase assay was performed. UT-34 and enzalutamide antagonized the wild-type AR with IC_{50} around 200 nmol/L. UT-34 inhibited the various mutant ARs (W741L, T877A, and F876L) comparably or with better IC_{50}. In contrast, enzalutamide was weaker in W741L by 5-fold, and behaved as a partial agonist in F876L AR (also partially antagonizes in the presence of androgens) as reported earlier (9, 14). IC_{50} value for enzalutamide in the antagonist mode could not be deduced due to its partial agonistic activity.

UT-34 downregulates T877A-AR and F876L-enzalutamide–resistant AR

As our objective was to develop degraders of the AR, we determined the effects of UT-34 on AR protein level in LNCaP cells and in enzalutamide-resistant MR49F cells as described in Fig. 2A and B. LNCaP or MR49F maintained in charcoal-stripped serum–containing medium were treated with a dose response of UT-34 in the presence of 0.1 nmol/L R1881 for 24 hours. Cells were harvested, protein extracted, and Western blotted for AR. While treatment of LNCaP cells with UT-34 resulted in a reduction of AR levels at 1,000 nmol/L (Fig. 2A, left), enzalutamide and bicalutamide failed to downregulate the AR in LNCaP cells (Fig. 2A, right). These effects occurred without an effect on AR mRNA expression (Fig. 2A, bar graph). Similar to parental LNCaP cells, MR49F cells treated with UT-34 exhibited a significant reduction in AR levels at around 1,000 nmol/L, which is comparable with that observed in LNCaP cells (Fig. 2B).

To demonstrate the selectivity of UT-34 to AR, the compound was tested in various cross-reactivity experiments. While UT-34 and enzalutamide failed to inhibit the transactivation of GR and mineralocorticoid receptor (Supplementary Table S1), UT-34 inhibited PR activity with a 4- to 5-fold weaker potency compared with the AR antagonistic activity.

To determine the degradation cross-reactivity of UT-34, we used various breast cancer cell lines that express AR and other steroid-hormone receptors. T47D that expresses ER and PR, but not AR, was used to evaluate the cross-reactivity of UT-34. T47D cells were maintained in serum-containing growth medium and treated with a dose response of UT-34 in the absence of R1881 and Western blot analysis for ER, PR, and actin was performed. UT-34 failed to downregulate the ER and PR protein levels (Fig. 2C). Although some reports suggest that T47D cells express AR (46, 47), our clone does not express AR.

To evaluate the cross-reactivity in a system that expresses AR, PR, and ER, we used ZR-75-1 breast cancer cells (48). Treatment of ZR-75-1 cells maintained in serum-containing growth medium with UT-34 resulted in downregulation of AR protein levels, but not ER or PR levels (Fig. 2D). Furthermore, in MDA-MB-453 breast cancer cells that express AR and GR (49, 50), UT-34 induced the downregulation of AR, but not GR (Supplementary Fig. S2A). This confirms that under similar condition, UT-34 is selective to AR and does not degrade other receptors.

UT-34 requires ubiquitin proteasome pathway to degrade the AR

To determine whether UT-34 promotes the ubiquitination of the AR, COS7 cells were transfected with AR and HA-tagged ubiquitin and treated with UT-155 or UT-34 in the presence of 0.1 nmol/L R1881. UT-155 was used as positive control in these experiments. Ubiquitin was immunoprecipitated using HA antibody and Western blot analysis for AR was performed. Western blot analysis for AR with nonimmunoprecipitated samples shows that both UT-155 and UT-34 downregulated the AR (Fig. 2E, input). When ubiquitin was immunoprecipitated and AR was detected, the AR was both mono- and polyubiquitinated in the presence of UT-34 and UT-155 (Fig. 2E). Similar results were also found in LNCaP cells treated with UT-155 or UT-34 (Fig. 2F). The proteasome inhibitor MG132, but not the HSP90 inhibitor 17AAG, enriched the ubiquitinated AR in cells treated with UT-34 or UT-155.

To further characterize the requirement of the proteasome pathway for UT-34 to downregulate the AR, LNCaP cells were treated with UT-34 and cycloheximide alone or in combination with a dose response of proteasome inhibitor bortezomib. UT-34 and cycloheximide combination downregulated the AR and this downregulation was reversed dose-dependently by bortezomib starting from 5 μmol/L (Fig. 2G). These results suggest that UT-34 requires ubiquitin proteasome pathway to degrade the AR.

We mutated the three known ubiquitin sites in AR (K311, K846, and K848) to arginine (R) and performed Western blots with protein extracts from cells transfected with wild-type and mutant ARs and treated with UT-34. UT-34 treatment facilitated the degradation of the wild-type and K-R–mutant ARs comparably (Fig. 2H), indicating that the known ubiquitin sites do not have a role in UT-34–dependent ubiquitin proteasome degradation. The effect of UT-34 on ubiquitination of the triple mutants needs to be evaluated.

To elucidate the signaling pathway that mediates the UT-34–dependent AR downregulation, we explored signaling pathways, p21-activated kinase (PAK), and protein kinase C (PKC) that have already been shown to promote AR ubiquitination. Phosphorylation of Ser^{578} by PAK has been demonstrated to be important for ubiquitin-dependent AR degradation. Moreover, because Ser^{578} is a substrate of both PAK and PKC (51, 52), we evaluated the role of these two pathways in UT-34–dependent degradation in LNCaP cells. Inhibition of PAK and PKC by small-molecule inhibitors, PF-3758309 (53) and chelerythrine chloride (54), respectively, failed to reverse the downregulation of AR by UT-34 (Supplementary Fig. S2B).

The ubiquitin E3 ligase that plays a role in AR's proteasomal degradation is MDM2 (52, 55). Using MDM2 siRNA, we evaluated the role of MDM2 in UT-34–dependent AR downregulation. LNCaP cells were transfected with MDM2 or nontargeting siRNAs and the expression of AR protein was determined by Western blot analysis. MDM2 siRNA failed to block the UT-34–dependent AR downregulation (Supplementary Fig. S2C). These results suggest that UT-34 downregulates AR through a mechanism independent of PAK, PKC, or MDM2.

UT-34 binds to AR-AF-1 domain

The steady-state fluorescence emission spectra for proteins results from the presence of aromatic amino acids, with tryptophan fluorescence making the dominant contribution. The AR-NTD polypeptide contains 19 tyrosine (Y), clustering in the

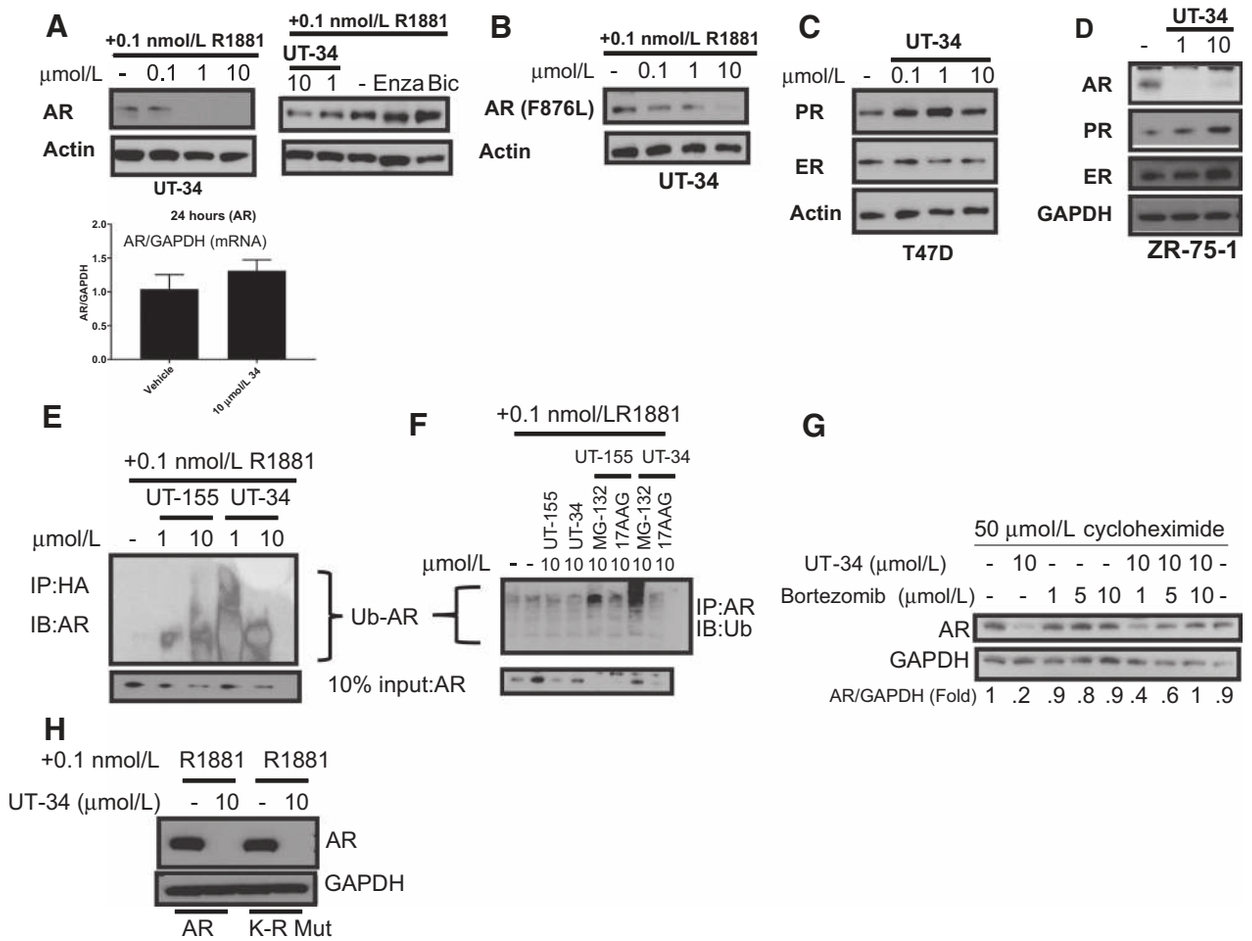

Figure 2.

UT-34 selectively degrades T877A and enzalutamide-resistant ARs. **A,** UT-34 destabilizes T877A AR. LNCaP cells were maintained in 1% charcoal-stripped serum–containing medium for two days. Cells were treated with the indicated doses of UT-34 or enzalutamide or bicalutamide (right; enzalutamide and bicalutamide were used at 10 μmol/L) in the presence of 0.1 nmol/L R1881 for 24 hours, protein was extracted, and Western blot analysis for AR and actin was performed. Bottom bar graph shows no effect of UT-34 on AR mRNA expression under the same experimental conditions. **B,** UT-34 destabilizes enzalutamide-resistant AR. Enzalutamide-resistant LNCaP cells (MR49F) were cultured and treated as indicated for LNCaP cells. Western blot analysis for AR and actin was performed with the protein extracts. **C** and **D,** UT-34 selectively degrades the AR. **C,** T47D cells maintained in full serum–containing medium were treated as indicated in the figure with UT-34. At 24 hours after treatment, cells were harvested, protein was extracted, and Western blot analysis for PR, ER, and actin was performed. **D,** ZR-75-1 cells were maintained in serum-containing growth medium and were treated as indicated in the figures for 48 hours with cells retreated after 24 hours. Cells were harvested and Western blot analysis for AR, PR, ER, and GAPDH was performed. **E,** UT-34 promotes ubiquitination of the AR. COS7 cells were transfected with 1 μg cmv-hAR and HA-ubiquitin. Cells were treated 48 hours after transfection for 6 hours. Cells were harvested, protein was extracted, and immunoprecipitation for HA and Western blot analysis for AR were performed. Ten percent of the protein extract was loaded as input. **F,** UT-34 promotes ubiquitination of the AR in LNCaP cells. LNCaP cells maintained in 1% charcoal-stripped serum–containing medium for two days were treated with UT-34 or UT-155 in the presence or absence of proteasome inhibitor, MG-132 and HSP-90 inhibitor, 17AAG, for 6 hours. Immunoprecipitation for AR was performed with the protein extract, and Western blot with mono- and polyubiquitin antibody was performed. **G,** UT-34 degrades the AR by proteasome pathway. LNCaP cells plated in growth medium were treated as indicated in the figure for 8 hours. Western blot analysis for AR and GAPDH was performed in the protein extracts. The blots were quantified and the numbers are represented under the Western image. **H,** Known ubiquitin sites do not play a role in UT-34–induced degradation of the AR. COS7 cells were transfected with 1 μg of wild-type AR or AR where three lysines (K311, K846, K848) were mutated to arginine (K to R). Cells were treated 24 hours after transfection for 24 hours, and Western blot analysis for AR and GAPDH was performed. Experiments were performed at least $n = 3$ and representative blots are shown here. PR, progesterone receptor; ER, estrogen receptor; IP, immunoprecipitation; IB, immunoblot (Western blot analysis); Ub, ubiquitin; cyclohex, cycloheximide-protein-synthesis inhibitor; Enza, enzalutamide; Bic, bicalutamide.

middle (amino acids 348–408) and toward the c-terminal region (amino acids 447–535), and four tryptophan residues (W399, 435, 503, and 527; Fig. 3A, top). Excitation at 278 nm results in fluorescence emission from tryptophan and tyrosine residues; in addition, there can be energy transfer from tyrosine to tryptophan. The spectrum thus provides information about the local conformation surrounding these residues (27, 56). The fluorescence spectrum for AR-AF1 is characterized by an emission maximum at 343 nm, due to the tryptophan residues ($W^{399, 435}$) and a shoulder at 309 nm, resulting from tyrosine emission (Fig. 3A, bottom left).

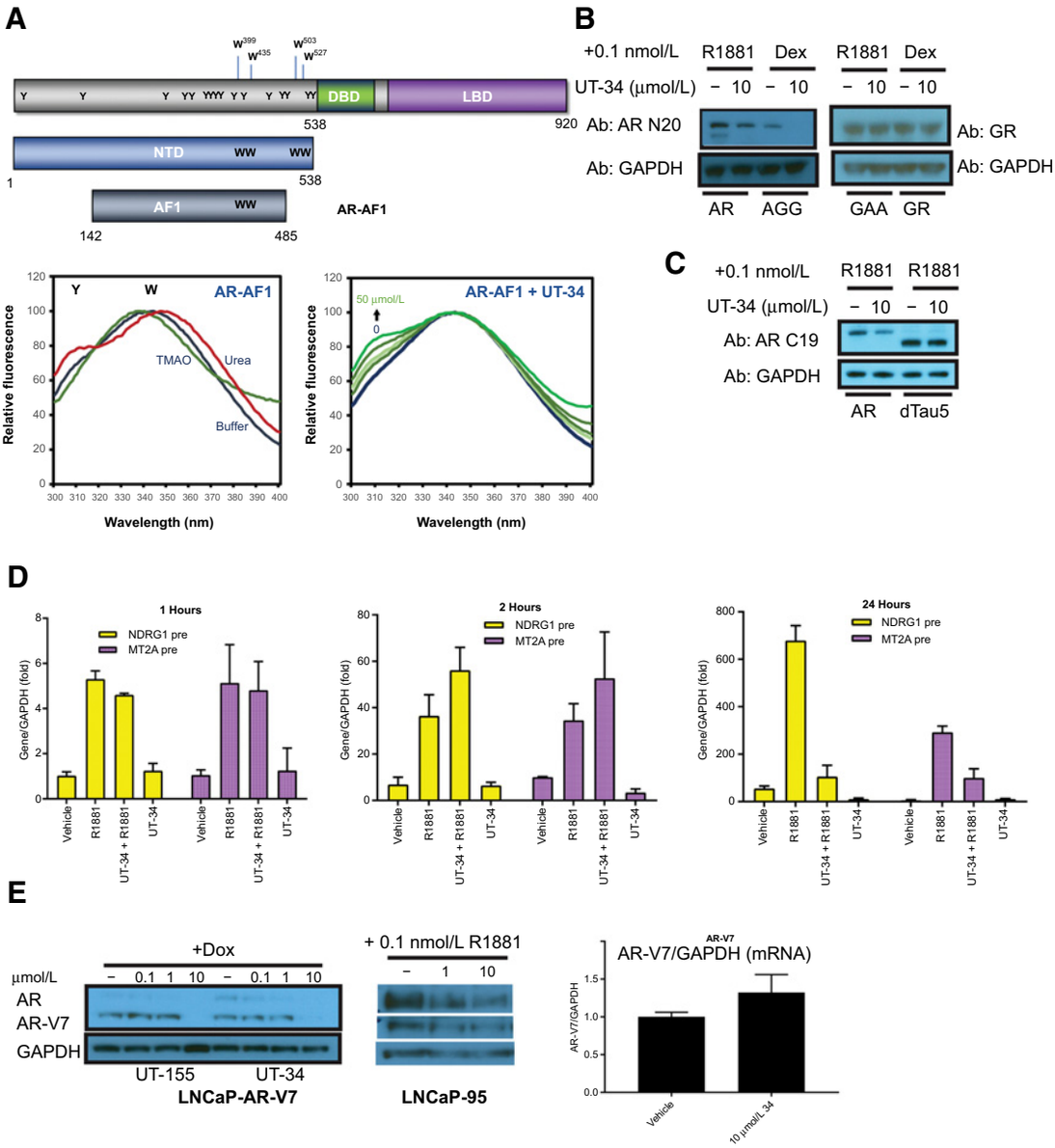

Figure 3.

UT-34 interacts with AR AF-1 domain. **A,** Top, Schematic representation of the full-length human AR and the AR-NTD and -AF1 polypeptide. The locations of tryptophan residues (399, 435, 503, and 527) and 19 tyrosines are indicated. Bottom left, steady-state fluorescence emission spectra for purified AR-AF1 (1 μmol/L) in buffer or the presence of the osmolyte TMAO or the denaturant urea. Emission maxima for tryptophan (W) and tyrosine (Y) are indicated. Bottom right, AR-AF-1–purified protein (1 μmol/L) and increasing concentrations of UT-34 were preincubated for at least 30 minutes and steady-state fluorescence was measured. The emission spectra were all corrected for buffer and presence of UT-34 and plotted relative to tryptophan emission maximum set to 100. **B,** UT-34 degrades chimeric protein that expresses AR-NTD. COS7 cells were transfected with 2.5 μg of the indicated constructs (AGG-AR-NTD, GR-DBD, and LBD; GAA-GR-NTD, AR-DBD, and LBD) and HA-ubiquitin. Cells were treated 24 hours after transfection and harvested 24 hours after treatment. Western blot analysis for AR and GAPDH (left) and GR and GAPDH (right) was performed. **C,** Tau-5 domain of the AR is important for UT-34–dependent degradation. COS7 cells were transfected with 2.5 μg of the indicated constructs and HA-ubiquitin, and Western blot analysis for AR using AR C19 antibody and GAPDH was performed. **D,** UT-34 does not inhibit early induction of NDRG1 and MT2A pre-mRNAs. LNCaP cells maintained in charcoal-stripped serum–containing medium for 2 days were treated as indicated in the figures in triplicates. Cells were pretreated with 10 μmol/L UT-34 for 30 minutes before treatment with 0.1 nmol/L R1881. Cells were harvested, RNA isolated, and the expression of various pre-mRNAs was measured at the indicated time-points. **E,** UT-34 degrades AR-SV. LNCaP-AR-V7 cells (LNCaP cells that stably express doxycycline-inducible AR-V7; left) or LNCaP-95 cells (middle) were maintained in charcoal-stripped serum–containing medium for 2 days. Doxycycline (10 ng/mL) was added to the LNCaP-AR-V7 cells during this period to induce the AR-V7 synthesis. After two days, medium was changed and the cells were treated with the indicated doses of UT-34 (UT-155 was used as a positive control in the left) for 24 hours. Protein was extracted and Western blot analysis for the AR and GAPDH was performed. Bar graph shows the lack of effect on AR-V7 mRNA in the presence of UT-34 under similar conditions. All the experiments were repeated three times, and a representative experiment is presented here. GR, glucocorticoid receptor; NTD, N terminus domain; DBD, DNA binding domain; Hin, Hinge; Dex, dexamethasone; AGG-AR NTD, GR DBD and LBD; GAA-GR NTD, AR DBD and LBD.

The folding or unfolding of AR-AF1/NTD has been investigated using TMAO, which has been shown to facilitate the folding of proteins into "native" conformations (56). In the presence of up to 3 mol/L TMAO there was blue shift in tryptophan emission maximum to 336 nm, and the shoulder due to tyrosine fluorescence was lost (Fig. 3A, bottom left). In contrast, in the presence of urea, the tryptophan emission "red shifts" to 351 nm and there is a clear peak for tyrosine emission. These results reflect the tryptophan residues becoming less or more solvent-exposed, respectively, and changes in the efficiency of energy transfer from tyrosine to tryptophan residues, consistent with the AR polypeptide folding/unfolding, respectively.

In the presence of UT-34, there are some striking changes in the steady-state emission spectra for both AR-AF1 and AR-NTD: all spectra were corrected for buffer and the presence of UT-34 alone. Increasing the concentration of UT-34 led to a peak at around 309 nm corresponding to tyrosine emission. Unlike our published data for UT-155, no clear quenching, reduction in the fluorescence emissions was observed in the presence of UT-34. Previously, quenching provided evidence for small-molecule binding (27, 29). The increase in the tyrosine signal is similar to that seen when AR-AF1/ NTD unfolds in the presence of urea, but there were no significant changes in the emission maximum for tryptophan (Fig. 3A, bottom right). Although difficult to interpret, it seems likely that UT-34 binding may lead to local unfolding of the receptor polypeptides (resulting in tyrosine emission), without altering the solvent exposure of the tryptophan residues. These results were reproduced with AR-NTD (Supplementary Fig. S2D).

As UT-34 binds to both LBD and AF-1 domains and also promotes degradation of the AR, we sought to determine the domain that is required for UT-34 to degrade the AR. Because UT-34 selectively promoted AR degradation and not the GR, AR-GR chimeric receptors were used to evaluate the domain(s) important for the degradation. AR, GR, or AR-GR chimeric receptors were transfected into cells and the cells were treated with UT-34 in the presence of the respective hormones. As shown earlier, UT-34 promoted the degradation of the full-length AR, but not the GR (Fig. 3B). UT-34 also promoted the degradation of the chimeric protein obtained from fusing AR-NTD to GR-DBD and -LBD (AGG), yet failed to promote degradation of the chimeric protein obtained from fusing GR-NTD to AR-DBD and AR-LBD (GAA). These results suggest that UT-34 potentially requires NTD to facilitate AR degradation (Fig. 3B).

To further refine the region in the AF-1 domain that is important for UT-34 to degrade the AR, a construct with the tau-5 domain deleted (tau-5–deleted AR) was used. COS7 cells were transfected with AR or tau-5–deleted AR, treated with vehicle or UT-34 for 48 hours, and a Western blot analysis was performed for AR and GAPDH. UT-34 caused the degradation of the full-length AR, but not the tau-5–deleted AR (Fig. 3C). Collectively, these data support UT-34 binding to the AR-NTD/AF-1 and the requirement of the Tau-5 region for the receptor degradation.

UT-34 does not inhibit the AR function by competitive antagonism

We then evaluated the early expression of pre-mRNAs in LNCaP cells treated with UT-34 in the presence or absence of R1881 (57). If UT-34 mediates its antagonistic effects through competitive antagonism, then these pre-mRNAs induced by R1881 as early as 30 minutes should be inhibited. However, if degradation is required for UT-34 to inhibit AR function, then early induction of the pre-mRNAs should not be inhibited as degradation will not be observed as early as 30 minutes to two hours. Treatment of LNCaP cells with 0.1 nmol/L R1881 increased both NDRG1 and MT2A pre-mRNAs by 1 hour and the increase was sustained at two and 24 hours (Fig. 3D). UT-34 failed to inhibit the expression of the pre-mRNA at 1 and two hours, yet inhibited the expression at 24 hours. These results indicate that UT-34 acts through AR degradation to elicit its effect, and competitive binding to the LBD, if any, may have no functional significance.

UT-34 promotes AR-V7 degradation

As the SARDs bind to the AF-1 domain and can promote AR-SV-degradation (27), we tested UT-34 in LNCaP cells that stably express inducible AR-V7 (30, 31). Consistent with our previous results (27), UT-155 caused the degradation of the AR and AR-V7 in this system. UT-34 treatment downregulated the AR and AR-V7, indicating that UT-34 is an effective degrader of both AR and AR-V7 (Fig. 3E). Similar findings were observed in LNCaP-95 cells that express AR and AR-V7 (Fig. 3E). These effects were observed without any effect on AR-V7 mRNA in LNCaP-ARV7 cells (Fig. 3E).

As UT-34 caused the downregulation of AR-V7, we evaluated the functional consequences of this downregulation. LNCaP-ARV7 cells were treated as indicated in Fig. 4A for 24 hours in the presence of 0.1 nmol/L R1881 or 10 ng/mL doxycycline. Cells were harvested and the expression of AR-target gene *FKBP5* and an AR-V7–specific gene *EDN2* (30, 31) was measured by real-time PCR. Doxycycline induced the expression of EDN2, which was inhibited by UT-34, but not by enzalutamide, while both enzalutamide and UT-34 inhibited the expression of R1881-induced *FKBP5* gene expression (Fig. 4A).

UT-34 differentially modulates AR–cofactor interaction compared with enzalutamide

To determine whether the properties of UT-34 are a result of a distinct interaction of AR with cofactors, we treated serum-starved LNCaP cells with 10 μmol/L UT-34, UT-155, or enzalutamide or vehicle in the presence of 1 nmol/L DHT. The cells were pretreated with the drugs or vehicle for 2 hours, followed by a 30-minute treatment with DHT. Protein extracts were subjected to microarray assay for real-time coregulator–nuclear receptor interaction (MARCoNI) assay where the interaction of the AR with 154 unique cofactor peptides from 66 cofactors was evaluated (43). UT-34 and UT-155 significantly modulated the AR–cofactor interaction (Fig. 4B, top). Although, the interaction between AR and cofactors in the presence of UT-155 and UT-34 was largely similar to enzalutamide (although with reduced potency), some differences were also observed (Fig. 4B, bottom panel and table). Differences in the interaction of AR with cofactors such as NCoR1 (corepressors) and TREF1 (coactivator) observed in SARD-treated samples were not observed in cells treated with enzalutamide. These results indicate that the conformation of AR in the presence of the SARDs is modestly distinct from the conformation in the presence of a competitive antagonist such as enzalutamide. The results from this cofactor profiling, as reflected by the conformation change, provide minimal mechanistic evidence for the UT-34's AR degradation effect. Further studies need to be performed to definitely determine whether the cofactor profile observed with UT-34 or UT-155 is an indicator of the conformation that is required to degrade the AR.

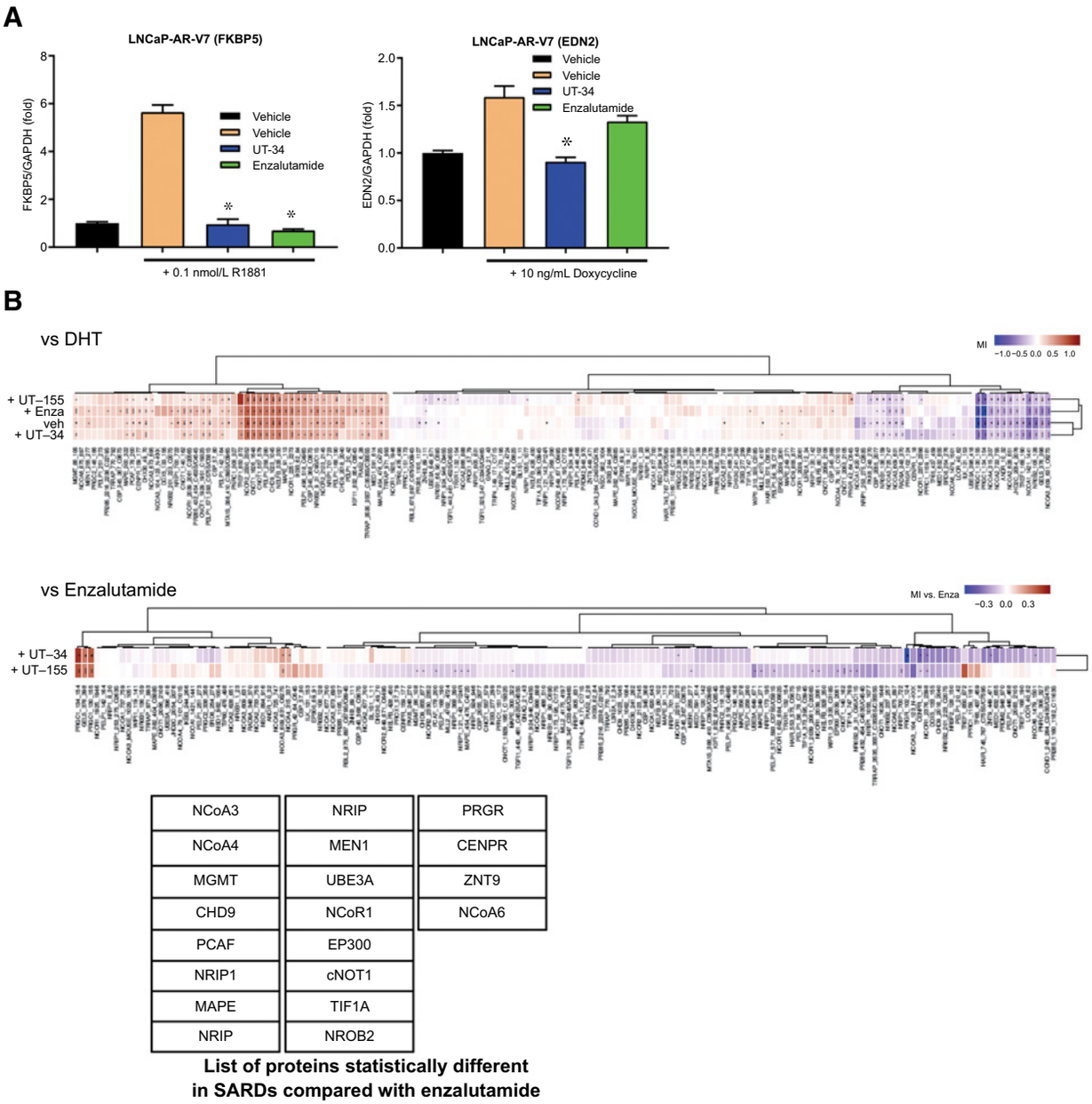

NCoA3	NRIP	PRGR
NCoA4	MEN1	CENPR
MGMT	UBE3A	ZNT9
CHD9	NCoR1	NCoA6
PCAF	EP300	
NRIP1	cNOT1	
MAPE	TIF1A	
NRIP	NROB2	

List of proteins statistically different in SARDs compared with enzalutamide

Figure 4.

UT-34 inhibits AR and AR-V7-target gene expression and induces distinct AR conformation. **A,** UT-34 inhibits AR and AR-V7-target gene expression. LNCaP-AR-V7 cells were maintained in charcoal-stripped serum–containing medium for 2 days. Cells were treated as indicated in the figure with 10 μmol/L of the compounds in the presence of 0.1 nmol/L R1881 or 10 ng/mL doxycycline (cells were pretreated with UT-34 for 30 minutes for combination with R1881 and for 24 hours for combination with doxycycline). Twenty-four hours after treatment initiation, the cells were harvested, RNA was isolated, and the expression of FKBP5 or EDN2 was determined by real-time PCR. Gene expression values were normalized to the expression of GAPDH. *, $P < 0.05$. Values are expressed as average ± SE ($n = 3$). **B,** UT-34 and UT-155 alter the conformation of the AR. LNCaP cells maintained in charcoal-stripped serum–containing medium for 2 days were treated with vehicle or 10 μmol/L of the indicated compounds in the presence of 1 nmol/L DHT (cells were pretreated for two hours). Cells were harvested 30 minutes after DHT treatment and the pellets were shipped to PamGene. AR was immunoprecipitated and cofactor profiling was done in accordance with the previously published protocols. List of proteins different in the SARD-treated samples from enzalutamide-treated samples is provided in the table below. Values represented are average of $n = 3$ technical replicates. Enza, enzalutamide; Veh, vehicle.

UT-34 antagonizes enzalutamide-resistant AR and inhibits the proliferation of enzalutamide-resistant MR49F cells

As UT-34 robustly antagonized and degraded wild-type, T877A, and enzalutamide-resistant ARs in transient transactivation and Western blot assays, we evaluated the effect of UT-34 on the function of ARs expressed in LNCaP or MR49F cells. LNCaP cells were maintained in charcoal-stripped FBS-containing medium for 48 hours and treated with a dose range of UT-34 or

enzalutamide in the presence of 0.1 nmol/L R1881. RNA was isolated and expression of AR target genes and growth was evaluated. Both the compounds inhibited the expression of PSA and FKBP5 and growth of LNCaP cells starting from 100 nmol/L with maximum effect observed at 10 μmol/L (Fig. 5A).

The experiment was also performed in MR49F cells that express F876L-mutant AR. UT-34, but not enzalutamide, inhibited the expression of *FKBP5* gene induced by R1881 (Fig. 5B). Concomitant to the gene expression studies, UT-34 inhibited the proliferation of MR49F cells, while as expected enzalutamide failed to inhibit their proliferation. The antiproliferative effects of UT-34 are selective to AR-positive prostate cancer cells, as UT-34 did not have any effect on the proliferation of AR-negative PC-3, COS7, and HEK-293 cells (Supplementary Fig. S3A).

UT-34 inhibits AR function and proliferation of an AR-amplified model (VCaP cells) and a PDX model

One of the mechanisms for CRPC development and for resistance to AR antagonists, bicalutamide in particular, is AR amplification (58–60). LNCaP cells ectopically overexpressing AR were used as a screening tool to discover and characterize enzalutamide and apalutamide (61). While bicalutamide was inactive or even behaved as an agonist in this model, enzalutamide was effective in reducing the LNCaP–AR cell proliferation and AR function (61). To test UT-34 in a model that has AR amplification, we used VCaP cells that endogenously expresses 10-fold higher AR than LNCaP cells (60). Earlier studies have shown that VCaP expresses 10-fold higher AR than parental LNCaP and 2–3 fold more than LNCaP-AR cells (60). Prior studies have also shown that bicalutamide is inactive or even functional as an agonist in this model (62, 63). Western blot analysis for AR expression in VCaP and LNCaP cells confirmed the AR amplification in VCaP cells compared with LNCaP cells (Fig. 5C). VCaP cells maintained in charcoal-stripped serum–containing medium for two days were treated with 3 and 10 μmol/L UT-34, enzalutamide, or bicalutamide in the presence of 0.1 nmol/L R1881 and the expression of AR target genes was measured (Fig. 5C). R1881 induced the expression of AR target genes, *FKBP5* and *TMPRSS2*, and this induction was inhibited by UT-34 and enzalutamide, but not by bicalutamide. Also, UT-34 and enzalutamide, but not bicalutamide, inhibited the proliferation of VCaP cells after 9 days of treatment (Fig. 5C). These results were confirmed in enzalutamide-resistant VCaP, MDVR cells (Supplementary Fig. S3B). These results suggest that, unlike bicalutamide, the effect of UT-34 is not weakened by AR amplification.

UT-34 was also evaluated in a PDX cell line PC346C that expresses AR at levels comparable with LNCaP (Fig. 5D). PC346C cells maintained in growth medium were treated with 3 and 10 μmol/L of UT-34 or enzalutamide and expression of AR target gene *FKBP5* was measured. UT-34 and enzalutamide inhibited FKBP5 expression, with UT-34 demonstrating a slightly better response than enzalutamide. Concurrent with the gene expression findings, UT-34 significantly inhibited the proliferation of PC346C cells.

UT-34 inhibits R1881-induced gene expression in MR49F cells

As UT-34 was effective in inhibiting the expression of FKBP5 in MR49F cells, we performed a microarray experiment to determine the effect of UT-34 on R1881-induced global gene expression (Fig. 5E, left). The resulting heatmap clearly illustrates that R1881 robustly altered the expression of approximately 700 genes. Most, if not all, of the genes regulated by R1881 were reversed by UT-34 almost to the level observed in vehicle-treated cells. The top genes that were inhibited by UT-34 are all known AR target genes such as *FKBP5*, *SNAI2*, *NDRG1*, and others. The results indicate that UT-34 is effective in reversing the R1881 effect in LNCaP cells expressing enzalutamide-resistant AR. Principal component analysis (PCA) shows that the UT-34–treated samples cluster with vehicle-treated samples, while R1881-treated samples clustered distinctly. When the genes that were not regulated by R1881 were plotted in a separate heatmap, the results show that UT-34 has no effect on these genes (Fig. 5E, right), indicating that UT-34 effects are highly selective to the AR pathway with no off-target effects.

Ingenuity Pathway Analysis (IPA) results indicate that the top four canonical pathways that were enriched in the differentially regulated genes were cholesterol-synthesizing pathways (Fig. 5F). While all genes in the pathway were upregulated by R1881 treatment, UT-34 efficiently reduced their expression to the vehicle-treated control levels. IPA also indicates that genes in genitourinary oncology pathways are differentially regulated, validating the model that was used to generate the gene expression data.

Drug metabolism and pharmacokinetic studies suggest that UT-34 is stable

Because of short half-life ($t_{1/2}$) of the first-generation SARDs, UT-155 and UT-69, in mouse liver microsomes [MLM; primary pharmacodynamic species; ref. 27), they had to be administered subcutaneously to obtain efficacy in preclinical models. Because CRPC is a chronic disease requiring prolonged treatment, orally bioavailable molecules are preferred for clinical development. Using MLM assay to determine the $t_{1/2}$ and intrinsic clearance, UT-34 was found to have a longer $t_{1/2}$ and lower intrinsic clearance than UT-155 (Supplementary Table S2). This suggests that UT-34 is an appropriate molecule for further development. Assessing the metabolism of UT-34 in rat liver microsome (RLM) and in human liver microsome (HLM), UT-34 was found to be highly stable and by at least 2- to 4-fold longer than in MLM.

To validate the *in vitro* data *in vivo*, the bioavailability of UT-34 at 6 and 24 hours after administration was determined in various strains of rats and mice (Supplementary Table S3). UT-34 was highly bioavailable in mice and rats at six hours. However, the serum concentration precipitously decreased at 24 hours in mice to almost undetectable levels, while higher levels in micromolar range were still observed in rats at 24 hours. A pharmacokinetic study was conducted in rats that were administered 100–1,000 mg/kg of UT-34 and the serum concentration was measured over a period of 24 hours. UT-34 was extremely stable in rats with $t_{1/2}$ for the 100 and 300 mg/kg doses undeterminable due to lack of 50% reduction by 24 hours and the serum concentrations in the range of 10–50 μmol/L (Supplementary Fig. S4A). These results are in concordance with the results observed in liver microsomes. Lower dose pharmacokinetics of UT-34 in rats also provided similar results with UT-34 demonstrating stability up to 24 hours (Supplementary Fig. S4B).

Pharmacodynamic and xenograft studies suggest that UT-34 is efficacious

To determine the efficacy of UT-34 *in vivo*, a Hershberger assay was performed in mice and rats (Supplementary Fig. S4C). Mice (left) were administered 20 or 40 mg/kg UT-34 or 30 mg/kg enzalutamide orally for 14 days. The animals were then sacrificed and the weight of the seminal vesicles was recorded.

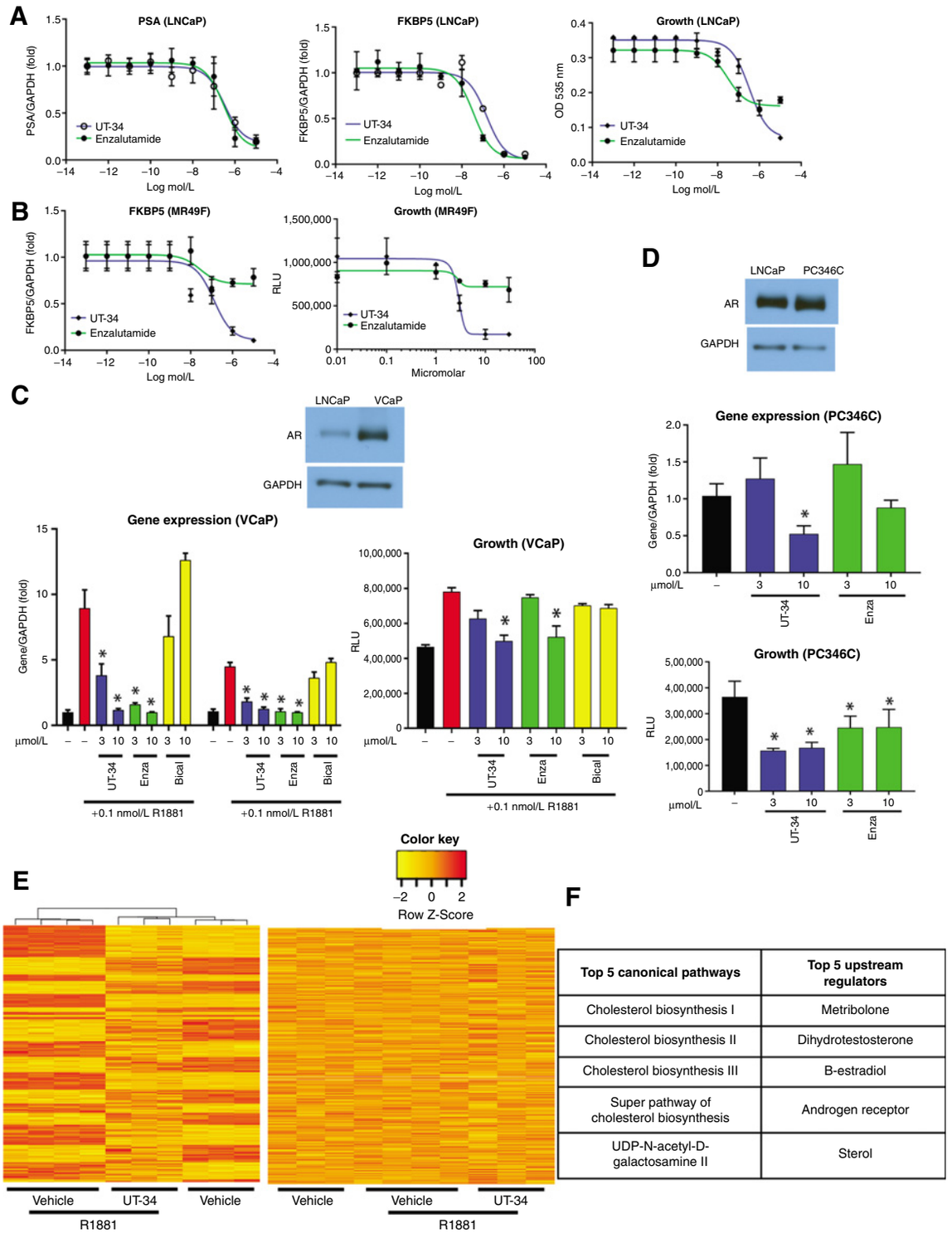

Top 5 canonical pathways	Top 5 upstream regulators
Cholesterol biosynthesis I	Metribolone
Cholesterol biosynthesis II	Dihydrotestosterone
Cholesterol biosynthesis III	B-estradiol
Super pathway of cholesterol biosynthesis	Androgen receptor
UDP-N-acetyl-D-galactosamine II	Sterol

Figure 5.

UT-34 inhibits enzalutamide-sensitive and -resistant AR-dependent gene expression and prostate cancer cell proliferation. **A,** UT-34 inhibits the expression of AR-target genes in LNCaP cells. LNCaP cells maintained in charcoal-stripped serum–containing medium for two days were treated with a dose response of UT-34 or enzalutamide in the presence of 0.1 nmol/L R1881. RNA was isolated 24 hours after treatment, and the expression of PSA and FKBP5 was quantified and normalized to GAPDH using real-time PCR primers and probes. For the growth assay (right), cells were maintained and treated as indicated above for the gene expression studies, but were treated for six days with medium change and retreatment after three days. (*Continued on the following page.*)

Enzalutamide was not dosed higher than 30 mg/kg due to its poor solubility. UT-34 at 20 and 40 mg/kg reduced the seminal vesicle weight by 10%–20% and 50%–60 %, respectively, while enzalutamide reduced the seminal vesicles weight by 50% (Supplementary Fig. S4C, left).

Sprague Dawley rats were dosed with 40 and 60 mg/kg of UT-34 orally and enzalutamide at 30 mg/kg for 14 days and the weight of the prostate was recorded. UT-34 reduced the prostate weight by approximately 70%–80%, while enzalutamide reduced the prostate weight by 40%–60%. This clearly shows that UT-34 is potent in shrinking the prostate potentially due to its antagonistic and degradation effects (Supplementary Fig. S4C, middle). Even after just four days of dosing, UT-34 reduced the prostate weight by nearly 50%, indicating its ability to antagonize the AR quickly *in vivo* and produce a PD effect (Supplementary Fig. S4C, right).

To evaluate the effect of UT-34 in an enzalutamide-resistant xenograft model, MR49F cells were implanted subcutaneously in NSG mice and once the tumors attained 100–200 mm^3, the animals were castrated and the tumors were allowed to regrow as CRPC. The animals were treated with 30 or 60 mg/kg UT-34 and the tumor volume was measured thrice weekly (Fig. 6A). UT-34 dose-dependently decreased the growth of the enzalutamide-resistant CRPC tumors with 60 mg/kg producing approximately 75% tumor growth inhibition. Tumor weights recorded at the end of the study also indicated that UT-34 reduced the tumor weights by approximately 60%–70% (Fig. 6A, right). Although the pharmacokinetic properties in mice were suboptimal compared with rats, UT-34 produced a marked effect on enzalutamide-resistant tumor growth.

UT-34 promotes regression of enzalutamide-sensitive and -resistant VCaP tumors in SRG rats

Because UT-34 is stable in rats compared with mice, we performed xenograft studies in immunocompromised rats (Hera Biolabs), using two models, enzalutamide-sensitive parental VCaP cells and enzalutamide acquired-resistant VCaP cells (MDVR). The rationale to choose VCaP over other models is a result of the relatively high AR expression (AR amplification), which is observed in a large percentage of men with CRPC (59). Cells were implanted in immunocompromised SRG rats and once the tumors reached a volume of 1,000–3,000 mm^3, the animals were castrated and the tumors were allowed to regrow as castration-resistant prostate cancer. Once the tumors reached >2,000 mm^3, the animals were randomized and treated orally with vehicle, 30 mg/kg enzalutamide, or 60 mg/kg UT-34. Tumor volume measurements indicated that while enzalutamide inhibited the growth of parental VCaP xenograft by >85%, UT-34 reduced the tumors to unmeasurable levels (Fig. 6B).

As expected, enzalutamide failed to inhibit the MDVR xenograft. The anticancer activity of UT-34 in this tumor model was comparable with that observed in the parental VCaP xenograft with UT-34 reducing the tumors to unmeasurable levels (Fig. 6C).

Because UT-34 reduced tumors to undetectable levels, we hypothesized that this could be due to its AR-degrading activity. Western blot analysis of MDVR tumors demonstrated AR degradation in UT-34–treated samples compared with vehicle-treated samples (Fig. 6C).

Previous studies with competitive AR antagonists were unable to demonstrate inhibition of tumors grown in intact mice. Because UT-34 is an orally bioavailable degrader, we were interested in testing the efficacy in intact models, where the animals were not castrated and the tumors were grown in the presence of circulating androgens. MDVR tumors grew robustly in SRG rats and the tumor-bearing animals were treated when the tumors attained >1,500 mm^3. One tumor in each group even attained 10,000 mm^3 when treatment was initiated. While the vehicle- and enzalutamide- treated tumors grew robustly, UT-34–treated tumors were reduced by >50% in less than 10–15 days after treatment initiation (Fig. 6D, individual tumors shown). We then measured serum PSA to determine whether tumor volume correlated with PSA levels. While PSA levels rose in vehicle-treated rats, UT-34 completely reduced serum PSA to undetectable levels after treatment initiation (Fig. 6D).

We subsequently conducted a dose response of UT-34 in intact SRG rats bearing MDVR tumors. UT-34 at 10 mg/kg inhibited the tumors by >50% and completely inhibited the tumors at 20 and 30 mg/kg doses (Fig. 6E). Both tumor weights and serum PSA at the end of the study clearly exhibited a dose-dependent inhibition by UT-34 (Fig. 6E). Measurement of drug concentration in the serum and tumor at necropsy, which was collected 24–30 hours after last dosing demonstrated UT-34 accumulation in both serum and tumor at over 1–3 μmol/L concentrations (Supplementary Fig. S4D). The steady-state drug concentration even 24 hours after the last dose is well above the IC_{50} values of UT-34 to inhibit the AR. IHC of vehicle- and UT-34–treated (30 mg/kg) specimens clearly indicated that UT-34 increased the apoptosis as measured by TUNEL assay and inhibited the proliferation as measured by Ki67 staining (Supplementary Fig. S4E). Taken together, these findings favorably point to the excellent antitumor activity of UT-34 in enzalutamide-sensitive and -resistant prostate cancers even in intact noncastrated animals. No

(*Continued.*) Sulforhodamine B (SRB) assay was performed to determine the number of viable cells. **B,** UT-34 inhibits the expression of AR-target genes in enzalutamide-resistant cells. Enzalutamide-resistant AR-expressing LNCaP cells (MR49F) were cultured and treated as indicated in **A**. RNA was isolated and the expression of AR-target gene FKBP5 was measured and normalized to GAPDH using real-time PCR primers and probe. Growth assay in MR49F cells was performed using CellTiter-Glo reagent. **C,** UT-34 inhibits VCaP AR function and cell proliferation. For Western blot analysis, protein from LNCaP and VCaP cells was extracted and Western blot analysis for AR and GAPDH was performed. Bottom left, VCaP cells were plated in growth medium. Medium was changed to 1% csFBS-containing medium and maintained in this medium for two days. Cells were treated for 24 hours, RNA was isolated, and expression of FKBP5 and TMPRSS2 was measured and normalized to GAPDH using real-time PCR. Bottom right, VCaP cells were plated in growth medium. Medium was changed to 1%csFBS containing medium and treated. Cells were retreated every third day and CellTiter-Glo assay was performed after 9 days. **D,** UT-34 inhibits PDX cell line PC346C AR function and cell proliferation. For Western blot analysis, protein from LNCaP and PC346C cells was extracted and Western blot for AR and GAPDH was performed. Middle, PC346C cells were plated in growth medium. Cells were treated for 24 hours in growth medium, RNA was isolated, and expression of FKBP5 was measured and normalized to GAPDH using real-time PCR. Bottom, PC346C cells were plated in growth medium and treated. Cells were retreated every third day and CellTiter-Glo assay was performed after 6 days. **E,** Gene expression array in MR49F indicates UT-34 reverses the expression of genes regulated by R1881. MR49F cells were maintained in charcoal-stripped serum–containing medium for 2 days and treated with vehicle, 0.1 nmol/L R1881 alone, or in combination with 10 μmol/L of UT-34. RNA was isolated 24 hours after treatment and hybridized to Clariom D microarray. Genes that were differentially expressed by 1.5-fold and $q < 0.05$ in R1881-treated samples compared with vehicle-treated samples are expressed in the heatmap to the left. The heatmap on the right shows the pattern of genes that were not regulated by R1881 ($n = 3$–4/group). **F,** Ingenuity Pathway Analysis (IPA) demonstrating the top 5 canonical pathways and upstream regulators that were enriched in the UT-34 datasets. Enza, enzalutamide; Bical, bicalutamide; *, $P < 0.05$; $n = 3$–4/group.

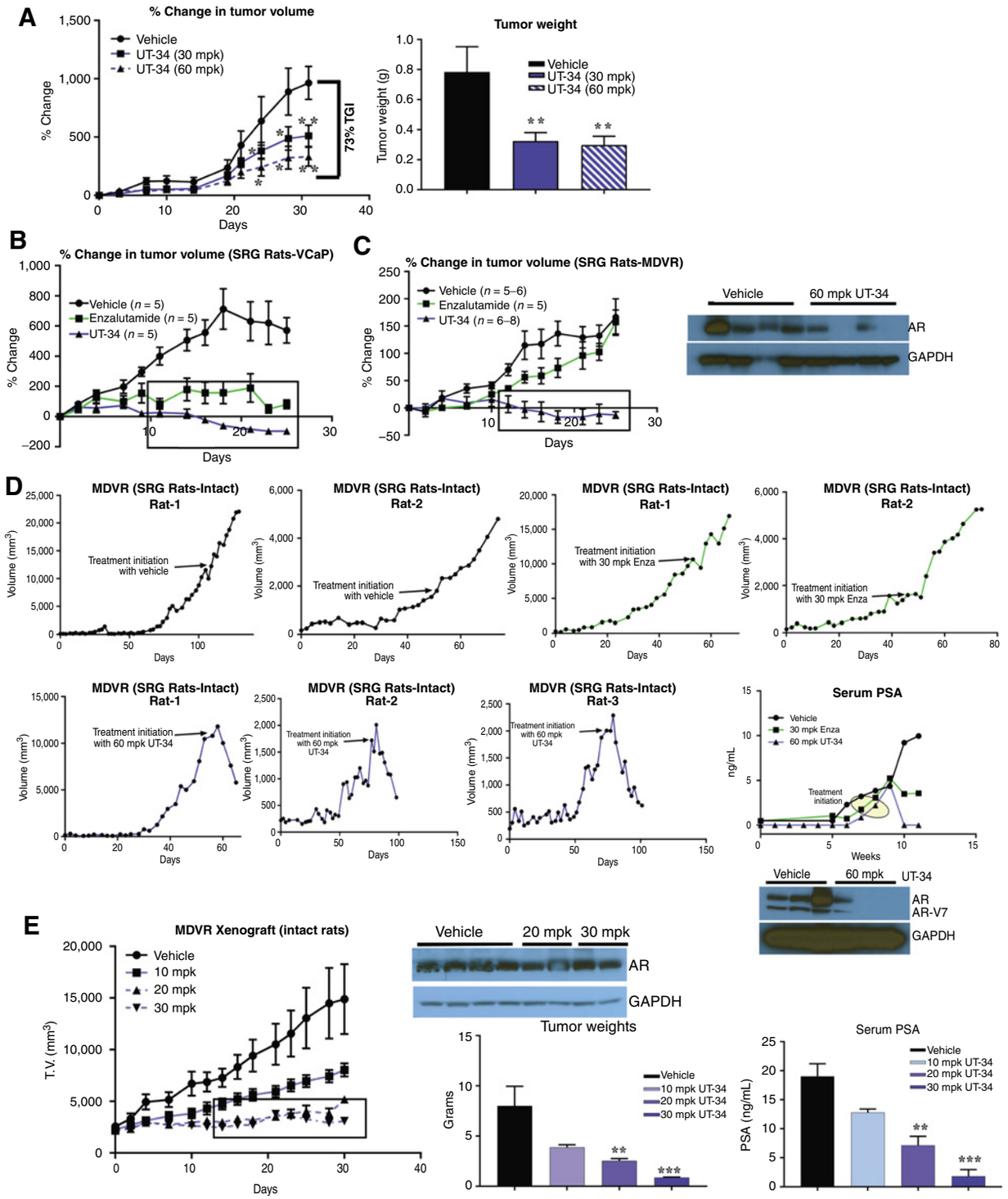

Figure 6.

UT-34 inhibits the growth of androgen-dependent and enzalutamide-refractory castration-resistant prostate cancer xenografts. **A,** UT-34 inhibits growth of enzalutamide-resistant xenograft. Enzalutamide-resistant LNCaP cells (MR49F) were implanted subcutaneously in NSG mice. Once the tumors reached 100–200 mm^3, the animals were castrated and the tumors were allowed to develop as castration-resistant tumors. Once the tumors reached 200–300 mm^3, the animals ($n = 8$–10/group) were randomized and treated orally with vehicle [DMSO:PEG-300 (15:85)] or the indicated doses of UT-34. Tumor volume was measured twice weekly. Animals were sacrificed on day 30 and tumor weights were recorded. Values are represented as average ± SE. *, $P < 0.05$; **, $P < 0.01$. **B,** UT-34 regresses tumors in immune-compromised rats. (*Continued on the following page.*)

visible changes in H&E staining were observed (Supplementary Fig. S5).

To determine whether the AR is degraded by UT-34 in intact conditions, we measured the AR expression by Western blot analysis in protein extracts from tumors (Fig. 6D). UT-34 robustly promoted degradation of the enzalutamide-resistant AR in intact condition (Fig. 6D), demonstrating that the degradation property translates *in vivo*. We also evaluated whether UT-34 promoted degradation of the AR at lower doses. Unfortunately, UT-34 failed to promote AR degradation at 30 mg/kg (Fig. 6E). This potentially suggests that higher serum and tumor concentrations are required to degrade the AR and that a tumor regression can be achieved only when the AR is degraded.

High doses of some receptor antagonists in certain cellular conditions could result in agonistic activity in artificial reporter assays. To ensure that UT-34 is a pure antagonist and does not have any agonistic activity at high doses, we tested UT-34 *in vivo* in castrated mice. Vehicle or UT-34 (100 mg/kg) was administered orally for 30 days to castrated mice, and seminal vesicles weights were recorded. Seminal vesicles are highly androgen-sensitive and any agonistic activity will increase its weight. Seminal vesicles weight normalized to body weight is expressed as percent change from vehicle control (Supplementary Fig. S4F). Even a high dose of UT-34 did not exhibit any agonistic activity as the normalized seminal vesicles weights in UT-34–treated group were comparable with weights of the vehicle-treated animals. Serum levels of UT-34 at the end of 30 days of dosing were in the range of 5–30 μmol/L (Supplementary Fig. S4F, right). These results confirm that UT-34 is a pure antagonist and does not have any agonistic properties *in vivo* even at higher doses.

UT-34 toxicity profile was acceptable

Because UT-34 possessed the required properties for a CRPC drug, we evaluated its toxicity profile. UT-34 was administered at 100, 300, and 600 mg/kg doses for seven days in Sprague Dawley rats and survival and gross pathology were monitored. UT-34 did not cause any death at 100 mg/kg dose, while deaths were encountered at 300 and 600 mg/kg doses. Gross pathology and histopathology findings suggest that the deaths in the higher dose groups were due to gastric irritation and inflammation, which could be potentially avoided by using enteric-coated capsules or salt forms of UT-34 (as UT-34 is a base). No other pathologic observations were detected at any dose. While several of the second-generation AR antagonists exhibit seizure potentials, mice treated with UT-34 did not have any seizure. In addition, UT-34 also does not have any significant cross-reactivity with GPCRs, kinases, or other nuclear receptors (Eurofin DiscoverX) and does not inhibit the hERG ion channel (Covance). These results suggest that UT-34 has a large safety margin and does not have off-target effects.

Discussion

Our results provide evidence for an orally bioavailable SARD that has the necessary drug-like properties for further clinical evaluation. UT-34 downregulated the AR and AR-V7 splice variant, antagonized enzalutamide-sensitive and resistant AR, inhibited proliferation of AR-amplified cells, and inhibited the growth of enzalutamide-resistant xenografts. UT-34 also possesses appropriate metabolism properties showing longer half-life, and shorter clearance in rat and human liver microsomes than in mouse liver microsomes. This suggests that UT-34 might require only once daily dosing for clinical efficacy.

UT-34 is effective in two models of enzalutamide-resistance (AR-LBD mutation and AR-V7 expression), which are common forms of resistance observed clinically. Although 30% of enzalutamide-resistant cancers do not respond at all, the remaining cancers eventually develop resistance after treatment. Mutations constitute only a small fraction of the resistance, while AR-SV development, intratumoral androgen synthesis, AR amplification, coactivators, and altered intracellular signaling pathways all contribute to resistance development. Degrading the AR and AR-SVs will block any AR activation by these contributing factors providing a significant advantage over existing therapeutics. Recently, two AR inhibitors, galeterone and EPI-506, failed in the clinic. After the approval of enzalutamide and abiraterone in 2012, no other drugs targeting the AR with distinct mechanism of action (apalutamide was approved recently, but it is structurally and functionally similar to enzalutamide) have been made available and patients have no treatment options with distinct mechanisms available to treat the new evolving forms of CRPC. Hence, these SARDs might provide a substantial advantage to the patients who relapse from enzalutamide.

We demonstrate that UT-34 promotes AR degradation through the ubiquitin proteasome pathway, the pathway by which most proteins are degraded. As AR degraders have not been successfully identified, thorough characterization of UT-34's mode of action is important. Unlike the ER degraders that act through the ER-LBD, UT-34 and its related compounds such as UT-155 act through the AR AF-1 domain in the N-terminus of the AR. UT-34 treatment resulted in mono- and poly-ubiquitinated AR. Also, inhibition of the proteasome pathway with bortezomib resulted in the reversal of AR degradation suggesting that the degradation takes place through proteasome pathway. Although recently available chimeric molecules such as PROTACs and SNIPERs have been shown to promote AR degradation (25, 64), these molecules are larger

(*Continued.*) VCaP prostate cancer cells (10 million) were mixed with 50% Matrigel and implanted subcutaneously in SRG immune-compromised rats. Once the tumors reached 1,000–3,000 mm^3, the animals were castrated and the tumors were allowed to regrow as CRPC. Once the tumors grew after castration to 2,000 mm^3, the animals were randomized ($n = 5$–6/group) and treated orally with vehicle [DMSO+PEG-300 (15:85)], 30 mg/kg enzalutamide, or 60 mg/kg UT-34. Tumor volume was measured thrice weekly. Lines in the box indicate that the tumors in the treated groups are significantly different at $P < 0.01$ to 0.001 from the vehicle group on the respective days. **C,** UT-34 regresses the growth of enzalutamide-resistant VCaP tumors (MDVR). Tumor studies were conducted as indicated in **B** in SRG rats ($n = 5$–6/group) with MDVR enzalutamide-resistant VCaP cells. For Western blot analysis, protein extracts from the tumors were fractionated on an SDS-PAGE and were Western blotted with AR and GAPDH antibodies. **D,** UT-34 regresses tumors in intact SRG rats. MDVR cells (10 million) were implanted subcutaneously. Once the tumors reached above 2,000 mm^3, the animals were randomized and treated orally with vehicle, 30 mg/kg enzalutamide, or 60 mg/kg UT-34. Individual animal data are presented. Serum PSA was measured using ELISA in three rats (one from each group) and is represented in the bottom right. Western blots for AR and GAPDH are shown in the bottom panel. **E,** UT-34 dose-dependently inhibits MDVR tumor growth in intact SRG rats. Xenograft studies were conducted in intact rats ($n = 5$/group) as indicated above with a dose response of UT-34. Tumor volume was measured thrice weekly. Lines in the box indicate that the tumors in the treated groups are significantly different at $P < 0.01$ to 0.001 from the vehicle group on the respective days. Tumor weights and serum PSA were recorded at the end of the treatment period. Western blot is shown as a panel. Mpk, mg/kg body weight; Enza, enzalutamide; SRG rats, Sprague Dawley-Rag2:IL2rg KO rats.

than the normally desired 500 Da size for clinically useful pharmacologic agents. Because UT-34 degrades the AR-SVs and the well-characterized ubiquitin sites in the AR did not play a role in AR degradation by UT-34 (Fig. 2H), UT-34 might act through novel ubiquitin sites in the AR-NTD that need to be identified.

This is the first time that an AR-targeting molecule has been shown to exhibit efficacy in xenograft models grown in intact (noncastrated) rodents. Because circulating testosterone levels are too high to be competed out with competitive antagonists, only noncompetitive antagonists or degraders can inhibit tumor growth in intact animals. The results observed in enzalutamide-resistant MDVR xenografts in intact rats are an *in vivo* confirmation that UT-34 might be a noncompetitive antagonist. Moreover, the dose response and higher dose xenograft studies also suggest that tumor regression was obtained when the AR is degraded and not when just antagonized. These results are the first evidence of efficacy of orally bioavailable small-molecule AR degraders.

The mechanism by which AR interacts with its cofactors in the presence of a degrader or in the presence of a molecule that binds to a distinct domain and that does not function as a competitive antagonist has not been elucidated. We conducted the study in LNCaP prostate cancer cells as opposed to the *in vitro* system followed by others (65). Both UT-34 and UT-155 promoted the interaction of several cofactors with the AR similar to that of a competitive antagonist enzalutamide, yet distinct interactions were observed in the presence of the two degraders. These interactions will be followed in the future with a library of compounds to validate the results.

Although the first-generation AR degraders, UT-155, UT-69, and others (27, 28), were more potent than UT-34 *in vitro* they were not orally bioavailable and their metabolism properties were not appropriate for drug development. Therefore, we had to compromise on the degradation and antagonist properties to improve the metabolism, which has resulted in a molecule that withstood various tests of efficacy and safety. Although a concern with AR-targeted drugs is seizure potential, UT-34 did not exhibit any seizure effects in rodents.

One of the intriguing properties of UT-34 is the difference in its pharmacokinetics between rats and mice. While the molecule was rapidly metabolized in mice, it was stable in rats. On the basis of the positive correlation between the liver microsome and pharmacokinetics properties in our dataset, we expect UT-34 to have similar, if not better, pharmacokinetic properties in humans. Although this species difference is an interesting observation, differences in pharmacokinetic properties between closely related species and between genders within a species have been reported previously (66, 67). The mechanism for such differences between closely related species or between genders within a species has not yet been elucidated.

UT-34 represents a new generation of orally bioavailable molecule that possesses necessary characteristics of AR degraders, warranting clinical development. We expect UT-34 to overcome enzalutamide resistance in the clinic without having to worry about some of the common safety problems.

Disclosure of Potential Conflicts of Interest

R. Houtman is an employee/paid consultant for PamGene. R.H. Getzenberg is an advisory board member/unpaid consultant for Veru Inc. D.D. Miller reports receiving commercial research grants from GTX. R. Narayanan reports receiving commercial research grants from and is an advisory board member/paid consultant for GTx, Inc. No potential conflicts of interest were disclosed by the other authors.

Authors' Contributions

Conception and design: S. Ponnusamy, Y. He, L.M. Pfeffer, R.H. Getzenberg, D.D. Miller, R. Narayanan
Development of methodology: S. Ponnusamy, Y. He, T. Thiyagarajan, Z. Du, D.D. Miller, R. Narayanan
Acquisition of data (provided animals, acquired and managed patients, provided facilities, etc.): S. Ponnusamy, R. Houtman, V. Bocharova, E. Fernandez, I.J. McEwan, R. Narayanan
Analysis and interpretation of data (e.g., statistical analysis, biostatistics, computational analysis): S. Ponnusamy, Y. He, R. Houtman, V. Bocharova, B.G. Sumpter, E. Fernandez, D. Johnson, Z. Du, Z. Du, L.M. Pfeffer, R.H. Getzenberg, I.J. McEwan, R. Narayanan
Writing, review, and/or revision of the manuscript: S. Ponnusamy, Y. He, D.-J. Hwang, R. Houtman, B.G. Sumpter, E. Fernandez, D. Johnson, L.M. Pfeffer, R.H. Getzenberg, I.J. McEwan, R. Narayanan
Administrative, technical, or material support (i.e., reporting or organizing data, constructing databases): S. Ponnusamy, T. Thiyagarajan, L.M. Pfeffer, R. Narayanan
Study supervision: S. Ponnusamy, L.M. Pfeffer, D.D. Miller, R. Narayanan
Other (synthesize, analyze and provide the designed chemical target): D.-J. Hwang

Acknowledgments

B.G. Sumpter acknowledges work performed at the Center for Nanophase Materials Sciences, a DOE Office of Science User Facility. V. Bocharova acknowledges Laboratory Directed Research and Development program of Oak Ridge National Laboratory, managed by UT-Battelle, LLC, for the U.S. Department of Energy. The work in this manuscript was funded by GTx, Inc.

The costs of publication of this article were defrayed in part by the payment of page charges. This article must therefore be hereby marked *advertisement* in accordance with 18 U.S.C. Section 1734 solely to indicate this fact.

Received May 6, 2019; revised July 1, 2019; accepted August 22, 2019; published first September 3, 2019.

References

1. Miller KD, Siegel RL, Lin CC, Mariotto AB, Kramer JL, Rowland JH, et al. Cancer treatment and survivorship statistics, 2016. CA Cancer J Clin 2016; 66:271–89.
2. de Bono JS, Logothetis CJ, Molina A, Fizazi K, North S, Chu L, et al. Abiraterone and increased survival in metastatic prostate cancer. N Engl J Med 2011;364:1995–2005.
3. Scher HI, Fizazi K, Saad F, Taplin ME, Sternberg CN, Miller K, et al. Increased survival with enzalutamide in prostate cancer after chemotherapy. N Engl J Med 2012;367:1187–97.
4. Smith MR, Kabbinavar F, Saad F, Hussain A, Gittelman MC, Bilhartz DL, et al. Natural history of rising serum prostate-specific antigen in men with castrate nonmetastatic prostate cancer. J Clin Oncol 2005;23:2918–25.
5. Chi KN, Hotte SJ, Yu EY, Tu D, Eigl BJ, Tannock I, et al. Randomized phase II study of docetaxel and prednisone with or without OGX-011 in patients with metastatic castration-resistant prostate cancer. J Clin Oncol 2010;28: 4247–54.
6. Scher HI, Beer TM, Higano CS, Anand A, Taplin ME, Efstathiou E, et al. Antitumour activity of MDV3100 in castration-resistant prostate cancer: a phase 1–2 study. Lancet 2010;375:1437–46.
7. Ryan CJ, Smith MR, de Bono JS, Molina A, Logothetis CJ, de Souza P, et al. Abiraterone in metastatic prostate cancer without previous chemotherapy. N Engl J Med 2013;368:138–48.
8. Nadiminty N, Tummala R, Liu C, Yang J, Lou W, Evans CP, et al. NF-kappaB2/p52 induces resistance to enzalutamide in prostate cancer:

role of androgen receptor and its variants. Mol Cancer Ther 2013;12:1629–37.
9. Korpal M, Korn JM, Gao X, Rakiec DP, Ruddy DA, Doshi S, et al. An F876L mutation in androgen receptor confers genetic and phenotypic resistance to MDV3100 (enzalutamide). Cancer Discov 2013;3:1030–43.
10. Antonarakis ES, Lu C, Wang H, Luber B, Nakazawa M, Roeser JC, et al. AR-V7 and resistance to enzalutamide and abiraterone in prostate cancer. N Engl J Med 2014;371:1028–38.
11. Lubahn DB, Joseph DR, Sullivan PM, Willard HF, French FS, Wilson EM. Cloning of human androgen receptor complementary DNA and localization to the X chromosome. Science 1988;240:327–30.
12. Yoshida T, Kinoshita H, Segawa T, Nakamura E, Inoue T, Shimizu Y, et al. Antiandrogen bicalutamide promotes tumor growth in a novel androgen-dependent prostate cancer xenograft model derived from a bicalutamide-treated patient. Cancer Res 2005;65:9611–6.
13. Clegg NJ, Wongvipat J, Joseph JD, Tran C, Ouk S, Dilhas A, et al. ARN-509: a novel antiandrogen for prostate cancer treatment. Cancer Res 2012;72:1494–503.
14. Balbas MD, Evans MJ, Hosfield DJ, Wongvipat J, Arora VK, Watson PA, et al. Overcoming mutation-based resistance to antiandrogens with rational drug design. Elife 2013;2:e00499.
15. Hornberg E, Ylitalo EB, Crnalic S, Antti H, Stattin P, Widmark A, et al. Expression of androgen receptor splice variants in prostate cancer bone metastases is associated with castration-resistance and short survival. PLoS One 2011;6:e19059.
16. Zhang G, Liu X, Li J, Ledet E, Alvarez X, Qi Y, et al. Androgen receptor splice variants circumvent AR blockade by microtubule-targeting agents. Oncotarget 2015;6:23358–71.
17. Cheng HH, Gulati R, Azad A, Nadal R, Twardowski P, Vaishampayan UN, et al. Activity of enzalutamide in men with metastatic castration-resistant prostate cancer is affected by prior treatment with abiraterone and/or docetaxel. Prostate Cancer Prostatic Dis 2015;18:122–7.
18. Mezynski J, Pezaro C, Bianchini D, Zivi A, Sandhu S, Thompson E, et al. Antitumour activity of docetaxel following treatment with the CYP17A1 inhibitor abiraterone: clinical evidence for cross-resistance? Ann Oncol 2012;23:2943–7.
19. Liu C, Zhu Y, Lou W, Cui Y, Evans CP, Gao AC. Inhibition of constitutively active Stat3 reverses enzalutamide resistance in LNCaP derivative prostate cancer cells. Prostate 2014;74:201–9.
20. Culig Z, Bartsch G, Hobisch A. Interleukin-6 regulates androgen receptor activity and prostate cancer cell growth. Mol Cell Endocrinol 2002;197:231–8.
21. McClelland RA, Manning DL, Gee JM, Anderson E, Clarke R, Howell A, et al. Effects of short-term antiestrogen treatment of primary breast cancer on estrogen receptor mRNA and protein expression and on estrogen-regulated genes. Breast Cancer Res Treat 1996;41:31–41.
22. Bihani T, Patel HK, Arlt H, Tao N, Jiang H, Brown JL, et al. Elacestrant (RAD1901), a selective estrogen receptor degrader (SERD), has antitumor activity in multiple ER+ breast cancer patient-derived xenograft models. Clin Cancer Res 2017;23:4793–804.
23. Watson PA, Chen YF, Balbas MD, Wongvipat J, Socci ND, Viale A, et al. Constitutively active androgen receptor splice variants expressed in castration-resistant prostate cancer require full-length androgen receptor. Proc Natl Acad Sci U S A 2010;107:16759–65.
24. Xu D, Zhan Y, Qi Y, Cao B, Bai S, Xu W, et al. Androgen receptor splice variants dimerize to transactivate target genes. Cancer Res 2015;75:3663–71.
25. Raina K, Lu J, Qian Y, Altieri M, Gordon D, Rossi AM, et al. PROTAC-induced BET protein degradation as a therapy for castration-resistant prostate cancer. Proc Natl Acad Sci U S A 2016;113:7124–9.
26. Tang YQ, Han BM, Yao XQ, Hong Y, Wang Y, Zhao FJ, et al. Chimeric molecules facilitate the degradation of androgen receptors and repress the growth of LNCaP cells. Asian J Androl 2009;11:119–26.
27. Ponnusamy S, Coss CC, Thiyagarajan T, Watts K, Hwang DJ, He Y, et al. Novel selective agents for the degradation of androgen receptor variants to treat castration-resistant prostate cancer. Cancer Res 2017;77:6282–98.
28. Hwang DJ, He Y, Ponnusamy S, Mohler ML, Thiyagarajan T, McEwan IJ, et al. A new generation of selective androgen receptor degraders: our initial design, synthesis, and biological evaluation of new compounds with enzalutamide-resistant prostate cancer activity. J Med Chem 2018;62:491–511.
29. Andersen RJ, Mawji NR, Wang J, Wang G, Haile S, Myung JK, et al. Regression of castrate-recurrent prostate cancer by a small-molecule inhibitor of the amino-terminus domain of the androgen receptor. Cancer Cell 2010;17:535–46.
30. Krause WC, Shafi AA, Nakka M, Weigel NL. Androgen receptor and its splice variant, AR-V7, differentially regulate FOXA1 sensitive genes in LNCaP prostate cancer cells. Int J Biochem Cell Biol 2014;54:49–59.
31. Shafi AA, Putluri V, Arnold JM, Tsouko E, Maity S, Roberts JM, et al. Differential regulation of metabolic pathways by androgen receptor (AR) and its constitutively active splice variant, AR-V7, in prostate cancer cells. Oncotarget 2015;6:31997–2012.
32. Hu R, Dunn TA, Wei S, Isharwal S, Veltri RW, Humphreys E, et al. Ligand-independent androgen receptor variants derived from splicing of cryptic exons signify hormone-refractory prostate cancer. Cancer Res 2009;69:16–22.
33. Toren PJ, Kim S, Pham S, Mangalji A, Adomat H, Guns ES, et al. Anticancer activity of a novel selective CYP17A1 inhibitor in preclinical models of castrate-resistant prostate cancer. Mol Cancer Ther 2015;14:59–69.
34. Marques RB, Aghai A, de Ridder CMA, Stuurman D, Hoeben S, Boer A, et al. High efficacy of combination therapy using PI3K/AKT inhibitors with androgen deprivation in prostate cancer preclinical models. Eur Urol 2015;67:1177–85.
35. Marques RB, Erkens-Schulze S, de Ridder CM, Hermans KG, Waltering K, Visakorpi T, et al. Androgen receptor modifications in prostate cancer cells upon long-term androgen ablation and antiandrogen treatment. Int J Cancer 2005;117:221–9.
36. Narayanan R, Coss CC, Yepuru M, Kearbey JD, Miller DD, Dalton JT. Steroidal androgens and nonsteroidal, tissue-selective androgen receptor modulator, S-22, regulate androgen receptor function through distinct genomic and nongenomic signaling pathways. Mol Endocrinol 2008;22:2448–65.
37. Yepuru M, Wu Z, Kulkarni A, Yin F, Barrett CM, Kim J, et al. Steroidogenic enzyme AKR1C3 is a novel androgen receptor-selective coactivator that promotes prostate cancer growth. Clin Cancer Res 2013;19:5613–25.
38. Scheller A, Hughes E, Golden KL, Robins DM. Multiple receptor domains interact to permit, or restrict, androgen-specific gene activation. J Biol Chem 1998;273:24216–22.
39. Callewaert L, Van Tilborgh N, Claessens F. Interplay between two hormone-independent activation domains in the androgen receptor. Cancer Res 2006;66:543–53.
40. Callewaert L, Verrijdt G, Haelens A, Claessens F. Differential effect of small ubiquitin-like modifier (SUMO)-ylation of the androgen receptor in the control of cooperativity on selective versus canonical response elements. Mol Endocrinol 2004;18:1438–49.
41. James AJ, Agoulnik IU, Harris JM, Buchanan G, Tilley WD, Marcelli M, et al. A novel androgen receptor mutant, A748T, exhibits hormone concentration-dependent defects in nuclear accumulation and activity despite normal hormone-binding affinity. Mol Endocrinol 2002;16:2692–705.
42. Reid J, Murray I, Watt K, Betney R, McEwan IJ. The androgen receptor interacts with multiple regions of the large subunit of general transcription factor TFIIF. J Biol Chem 2002;277:41247–53.
43. Houtman R, de Leeuw R, Rondaij M, Melchers D, Verwoerd D, Ruijtenbeek R, et al. Serine-305 phosphorylation modulates estrogen receptor alpha binding to a coregulator peptide array, with potential application in predicting responses to tamoxifen. Mol Cancer Ther 2012;11:805–16.
44. Cato L, de Tribolet-Hardy J, Lee I, Rottenberg JT, Coleman I, Melchers D, et al. ARv7 represses tumor-suppressor genes in castration-resistant prostate cancer. Cancer Cell 2019;35:401–13.
45. Narayanan R, Yepuru M, Szafran AT, Szwarc M, Bohl CE, Young NL, et al. Discovery and mechanistic characterization of a novel selective nuclear androgen receptor exporter for the treatment of prostate cancer. Cancer Res 2010;70:842–51.
46. Buchanan G, Birrell SN, Peters AA, Bianco-Miotto T, Ramsay K, Cops EJ, et al. Decreased androgen receptor levels and receptor function in breast cancer contribute to the failure of response to medroxyprogesterone acetate. Cancer Res 2005;65:8487–96.
47. Tilley WD, Marcelli M, McPhaul MJ. Expression of the human androgen receptor gene utilizes a common promoter in diverse human tissues and cell lines. J Biol Chem 1990;265:13776–81.

48. Mitchell S, Abel P, Madaan S, Jeffs J, Chaudhary K, Stamp G, et al. Androgen-dependent regulation of human MUC1 mucin expression. Neoplasia 2002;4:9–18.
49. Robinson JL, Macarthur S, Ross-Innes CS, Tilley WD, Neal DE, Mills IG, et al. Androgen receptor driven transcription in molecular apocrine breast cancer is mediated by FoxA1. EMBO J 2011;30:3019–27.
50. Hartig PC, Bobseine KL, Britt BH, Cardon MC, Lambright CR, Wilson VS, et al. Development of two androgen receptor assays using adenoviral transduction of MMTV-luc reporter and/or hAR for endocrine screening. Toxicol Sci 2002;66:82–90.
51. Patek S, Willder J, Heng J, Taylor B, Horgan P, Leung H, et al. Androgen receptor phosphorylation status at serine 578 predicts poor outcome in prostate cancer patients. Oncotarget 2017;8:4875–87.
52. Liu T, Li Y, Gu H, Zhu G, Li J, Cao L, et al. p21-Activated kinase 6 (PAK6) inhibits prostate cancer growth via phosphorylation of androgen receptor and tumorigenic E3 ligase murine double minute-2 (Mdm2). J Biol Chem 2013;288:3359–69.
53. Civiero L, Cogo S, Kiekens A, Morganti C, Tessari I, Lobbestael E, et al. PAK6 phosphorylates 14–3–3gamma to regulate steady state phosphorylation of LRRK2. Front Mol Neurosci 2017;10:417.
54. Eckly-Michel AE, Le Bec A, Lugnier C. Chelerythrine, a protein kinase C inhibitor, interacts with cyclic nucleotide phosphodiesterases. Eur J Pharmacol 1997;324:85–8.
55. Vummidi Giridhar P, Williams K, VonHandorf AP, Deford PL, Kasper S. Constant degradation of the androgen receptor by MDM2 conserves prostate cancer stem cell integrity. Cancer Res 2019;79:1124–37.
56. Reid J, Kelly SM, Watt K, Price NC, McEwan IJ. Conformational analysis of the androgen receptor amino-terminal domain involved in transactivation. Influence of structure-stabilizing solutes and protein-protein interactions. J Biol Chem 2002;277:20079–86.
57. Trevino LS, Bolt MJ, Grimm SL, Edwards DP, Mancini MA, Weigel NL. Differential regulation of progesterone receptor-mediated transcription by CDK2 and DNA-PK. Mol Endocrinol 2016;30:158–72.
58. Linja MJ, Savinainen KJ, Saramaki OR, Tammela TL, Vessella RL, Visakorpi T. Amplification and overexpression of androgen receptor gene in hormone-refractory prostate cancer. Cancer Res 2001;61:3550–5.
59. Visakorpi T, Hyytinen E, Koivisto P, Tanner M, Keinanen R, Palmberg C, et al. *In vivo* amplification of the androgen receptor gene and progression of human prostate cancer. Nat Genet 1995;9:401–6.
60. Waltering KK, Helenius MA, Sahu B, Manni V, Linja MJ, Janne OA, et al. Increased expression of androgen receptor sensitizes prostate cancer cells to low levels of androgens. Cancer Res 2009;69:8141–9.
61. Tran C, Ouk S, Clegg NJ, Chen Y, Watson PA, Arora V, et al. Development of a second-generation antiandrogen for treatment of advanced prostate cancer. Science 2009;324:787–90.
62. Kawata H, Arai S, Nakagawa T, Ishikura N, Nishimoto A, Yoshino H, et al. Biological properties of androgen receptor pure antagonist for treatment of castration-resistant prostate cancer: optimization from lead compound to CH5137291. Prostate 2011;71:1344–56.
63. Makkonen H, Kauhanen M, Jaaskelainen T, Palvimo JJ. Androgen receptor amplification is reflected in the transcriptional responses of vertebral-cancer of the prostate cells. Mol Cell Endocrinol 2011;331:57–65.
64. Shibata N, Nagai K, Morita Y, Ujikawa O, Ohoka N, Hattori T, et al. Development of protein degradation inducers of androgen receptor by conjugation of androgen receptor ligands and inhibitor of apoptosis protein ligands. J Med Chem 2018;61:543–75.
65. Pollock JA, Wardell SE, Parent AA, Stagg DB, Ellison SJ, Alley HM, et al. Inhibiting androgen receptor nuclear entry in castration-resistant prostate cancer. Nat Chem Biol 2016;12:795–801.
66. Czerniak R. Gender-based differences in pharmacokinetics in laboratory animal models. Int J Toxicol 2001;20:161–3.
67. Chang SC, Das K, Ehresman DJ, Ellefson ME, Gorman GS, Hart JA, et al. Comparative pharmacokinetics of perfluorobutyrate in rats, mice, monkeys, and humans and relevance to human exposure via drinking water. Toxicol Sci 2008;104:40–53.